

# Conformal causal inference for cluster randomized trials: model-robust inference without asymptotic approximations

Bingkai Wang<sup>1</sup>, Fan Li<sup>2,3</sup>, and Mengxin Yu<sup>4</sup>

<sup>1</sup>Department of Biostatistics, University of Michigan, Ann Arbor, MI, USA

<sup>2</sup>Department of Biostatistics, Yale School of Public Health, New Haven, CT, USA

<sup>3</sup>Center for Methods in Implementation and Prevention Science, Yale School of Public Health,  
New Haven, CT, USA

<sup>4</sup>Department of Statistics and Data Science, University of Pennsylvania, Philadelphia, PA, USA

## Abstract

In the analysis of cluster randomized trials, two typical features are that individuals within a cluster are correlated and that the total number of clusters can sometimes be limited. While model-robust treatment effect estimators have been recently developed, their asymptotic theory requires the number of clusters to approach infinity, and one often has to empirically assess the applicability of those methods in finite samples. To address this challenge, we propose a conformal causal inference framework that achieves the target coverage probability of treatment effects in finite samples without the need for asymptotic approximations. Meanwhile, we prove that this framework is compatible with arbitrary working models, including machine learning algorithms leveraging baseline covariates, possesses robustness against arbitrary misspecification of working models, and accommodates a variety of within-cluster correlations. Under this framework, we offer efficient algorithms to make inferences on treatment effects at both the cluster and individual levels, applicable to user-specified covariate subgroups and two types of test data. Finally, we demonstrate our methods via simulations and a real data application based on a cluster randomized trial for treating chronic pain.

*Keywords:* Cluster randomized experiments; conformal prediction; machine learning; individual-level treatment effect; cluster-level treatment effect; finite-sample coverage.

# 1 Introduction

Cluster randomized trials (CRTs, [Murray et al., 1998](#)) represent a type of randomized trials where the treatment is assigned at the cluster level. The clusters can be schools, hospitals, or villages, and the associated treatment can be new healthcare practices or policy innovations, among others. In recent years, CRTs have become increasingly popular in pragmatic clinical trials to evaluate the treatment effect in routine practice conditions. Compared to trials with individual randomization, CRTs offer enhanced cost-effectiveness, effectively mitigate the risk of treatment contamination, and facilitate the evaluation of interventions that are naturally implemented at the cluster level.

In analyzing CRTs, there has been an increasing interest in pursuing model-robust inference in lieu of conventional model-based inference, aiming to provide stronger statistical guarantees for estimating targeted causal estimands ([Su and Ding, 2021](#); [Balzer et al., 2023](#); [Wang et al., 2023](#)). Briefly, *model robustness* means that the validity of inference does not rely on the correct specification of the selected working model. For example, when a linear mixed model is used to construct a confidence interval for the average treatment effect, we aim to achieve the target coverage probability even when the working model is arbitrarily misspecified ([Wang et al., 2021](#)). Model robustness is a desirable property since the true and potentially complex data-generating distribution is unknown, and thus, any working model can be misspecified. For example, the outcome may be a nonlinear function of covariates, follow a non-normal distribution, and have a complex covariate-dependent correlation structure. Because these complexities cannot be ruled out in practice, it is almost impossible to pre-specify a working model that perfectly captures the true data-generating process, thereby rendering model-robust inference attractive for improving the rigor and precision in analyzing CRTs.

For model-robust inference in CRTs, model-assisted regression and permutation inference represent two typical approaches, but they both have important limitations. Model-assisted regression requires the asymptotic theory assuming the number of clusters (i.e., the number of independent units, due to unknown intra-cluster correlation) approaches infinity ([Balzer](#)

et al., 2016; Su and Ding, 2021; Wang et al., 2021; Balzer et al., 2023; Wang et al., 2023). Nonetheless, its practical usefulness for CRTs may be constrained by the limited number of clusters typically available in such studies. For an example context, Ivers et al. (2011) reviewed 300 CRTs published between 2000 and 2008 across disciplines, and found that at least 50% randomized no more than 21 clusters, which can be too small for the asymptotic results to apply. Alternatively, the permutation test can achieve model-robust finite-sample hypothesis testing for the sharp null (Small et al., 2008; Zhang et al., 2012; Ding and Keele, 2018). However, the sharp null may be overly restrictive—that is, even when a permutation test rejects the sharp null, the average treatment effect may still be zero due to treatment effect heterogeneity. Besides, the computation for permutation-based confidence intervals is often non-trivial (Rabideau and Wang, 2021). To this end, improvement for model-robust inference in CRTs that can achieve finite-sample validity with minimal assumptions and efficiently leverage covariate information is much needed.

In this article, we integrate conformal prediction, as conceptualized by Vovk et al. (2005), to perform model-robust causal inference for CRTs. In the prediction context, conformal prediction aims to construct a covariate-based interval (using an arbitrary working model) such that the outcome resides in this interval with a desired probability, e.g., 95%. Remarkably, this coverage probability is model-robust even in finite samples, provided that the data distribution is exchangeable among individuals. Given that its model robustness is independent of any asymptotic regimes, conformal prediction effectively solves the analytical challenges with a limited number of independent units, making it a promising paradigm for analyzing CRTs. Although conformal prediction has been connected with causal inference for non-clustered data (Lei and Candès, 2021; Yang et al., 2022; Qiu et al., 2022; Yin et al., 2022; Alaa et al., 2023; Jin et al., 2023), conformal causal inference for multilevel data has not been previously investigated and poses new challenges. First, CRT data may not be exchangeable at the individual level because the *intra*-cluster correlation can be much larger than the *inter*-cluster correlation, causing non-exchangeability for individuals from different clusters. As a result, the existing theory of conformal causal inference cannot be directly

applied without essential modifications. Second, the multilevel data structure of CRTs implies more than one treatment effect at different levels, whose magnitude and interpretation can differ (Kahan et al., 2023), and conformal causal inference requires adaptation to target each treatment effect. Third, while existing results for conformal causal inference focus on the marginal interpretation over the entire study population, inferring treatment effects among certain subpopulations can lead to more informative and targeted interpretations, representing a valuable extension for inference in CRTs.

The principal contribution of this article is to propose a conformal causal inference framework tailored for CRTs that address the aforementioned challenges. Specifically, given any working model, we provide algorithms to construct prediction intervals for both the cluster-level and individual-level treatment effect and prove their finite-sample model robustness under minimal assumptions. The cluster-level treatment effect assesses the impact of treatment on a new cluster as a whole, while the individual-level treatment effect focuses on the impact experienced by any given individual within a new cluster: both treatment effects can be meaningful for decision-making depending on the scientific questions. Furthermore, we extend our methods to perform subgroup analysis, that is, achieving the desired coverage probability conditioning on any set with a positive measure in the covariate data space. Throughout, the proposed method allows for the integration of machine learning algorithms as a base learner for the outcome given baseline covariates, in order to narrow the prediction intervals for the target treatment effects without compromising validity in finite samples.

## 2 Notation, assumptions, and targets of inference

### 2.1 Potential outcomes framework

We consider a CRT with  $m$  clusters, and each cluster  $i$ ,  $i = 1, \dots, m$ , includes  $N_i$  individuals. At the cluster level, we define  $A_i$  as a binary treatment indicator ( $A_i = 1$  for treatment and  $A_i = 0$  for control) and  $R_i$  as a vector of cluster-level covariates, such as the geographical location of the cluster. For each individual  $j = 1, \dots, N_i$  in cluster  $i$ , we denote  $Y_{ij}$  as their

observed outcome,  $X_{ij}$  as a vector of individual-level baseline covariates. The observed data for each cluster are  $O_i = \{(Y_{ij}, A_i, X_{ij}, R_i) : j = 1, \dots, N_i\}$ . To proceed, we adopt the potential outcomes framework and define  $Y_{ij}(a)$  as the potential outcome for individual  $j$  of cluster  $i$  had cluster  $i$  been assigned  $A_i = a$  for  $a = 0, 1$ . We assume consistency such that  $Y_{ij} = A_i Y_{ij}(1) + (1 - A_i) Y_{ij}(0)$ . Denoting the complete data vector for each cluster as  $W_i = \{(Y_{ij}(1), Y_{ij}(0), X_{ij}, R_i) : j = 1, \dots, N_i\}$ , we make the following structural assumptions on  $(W_1, \dots, W_m)$  and the assignment vector  $(A_1, \dots, A_m)$ .

**Assumption 1** (*Random sampling of clusters*). Each  $W_i$  is an independent, identically distributed sample from an unknown distribution  $\mathcal{P}^W$  on  $W = \{(Y_{\bullet,j}(1), Y_{\bullet,j}(0), X_{\bullet,j}, R) : j = 1, \dots, N\}$ , where the subscript ‘ $\bullet, j$ ’ represents the  $j$ -th individual in  $W$ .

**Assumption 2** (*Cluster randomization*). Each  $A_i$  is an independent, identically distributed sample from a Bernoulli distribution  $\mathcal{P}^A$  with  $P(A = 1) = \pi$  for a known constant  $\pi \in (0, 1)$ . Furthermore,  $\mathcal{P}^A$  is independent of  $\mathcal{P}^W$ .

**Assumption 3** (*Within-cluster exchangeability*). For any permutation map  $\sigma$  on the index set  $\{1, \dots, N\}$ , the vector  $\{W_{\bullet,1}, \dots, W_{\bullet,N}\}$  has the same distribution as  $\{W_{\bullet,\sigma(1)}, \dots, W_{\bullet,\sigma(N)}\}$  conditioning on  $N$ , where  $W_{\bullet,j} = (Y_{\bullet,j}(1), Y_{\bullet,j}(0), X_{\bullet,j}, R)$ .

Assumption 1 states that each observed cluster is an independent draw from the same distribution and is standard for drawing inference under a sampling-based framework. To accommodate the difference in the dimension of  $W_i$  across clusters, we can decompose  $\mathcal{P}^W = \mathcal{P}^{W|N} \times \mathcal{P}^N$  such that  $N_i$  is first sampled from  $\mathcal{P}^N$  and  $W_i$  is then generated following  $\mathcal{P}^{W|N}$ . Assumption 2 often holds by design. Assumption 3 states that the joint distribution of individuals in a cluster is invariant to permutations of the index of individuals. Importantly, this assumption still allows heterogeneous outcome correlation after conditioning on covariates, which means the conditional correlation of  $Y_{\bullet,j}$  and  $Y_{\bullet,j'}$  can arbitrarily depend on  $X_{\bullet,j}$  and  $X_{\bullet,j'}$  through a shared covariance function across  $(j, j')$  pairs; see [Crespi et al. \(2009\)](#) for an example data-generating process in the context of second-order generalized estimating equations. As a result, Assumption 3 encompasses a wide variety of within-cluster

correlation structures and is not to be confused with the restrictive random-intercept model assumption (which implies an overly simplistic constant intracluster correlation and is a special case of Assumption 3). Of note, Assumption 3 is weaker than those in Balzer et al. (2016) and Benitez et al. (2023), which further assumes conditional independence among individual-level observations within each cluster for asymptotic inference.

## 2.2 Conventional target of inference goals in CRTs

Conventionally, statistical inference for CRTs focuses on the average treatment effect. For example, when the interest lies in the cluster-average treatment effect  $\Delta_C = E[\bar{Y}(1) - \bar{Y}(0)]$  with  $\bar{Y}(a) = \frac{1}{N} \sum_{j=1}^N Y_{\bullet,j}(a)$ , one important inferential target is to construct a confidence interval  $\widehat{CI}_m$  satisfying  $P(\Delta_C \in \widehat{CI}_m) = 1 - \alpha$  with  $\alpha$  being a pre-specified type I error rate. Often in practice,  $\widehat{CI}_m$  leverages baseline covariates to sharpen the interval and reduce the type II error rate. Despite its simple form, this objective may be difficult without parametric modeling assumptions, such as linear mixed models or Bayesian methods. However, parametric assumptions implicitly put strong constraints on the space of possible data-generating distributions and, therefore, can be violated under non-linearity or non-normality, among others. To overcome this challenge, Su and Ding (2021) and Wang et al. (2023) developed asymptotic theory that guarantees a weaker result,  $\lim_{m \rightarrow \infty} P(\Delta_C \in \widehat{CI}_m) = 1 - \alpha$ , which states that the target coverage probability of a model-assisted confidence interval is achievable as the number of clusters approaches infinity, even under arbitrary working model misspecification. Nonetheless, this modified inferential target may not be fully satisfactory since the number of clusters  $m$  is often limited in CRTs.

## 2.3 Conformal causal inference in CRTs

For finite-sample inference that is robust to model misspecification, we propose an alternative inference target defined as follows. Given any  $\alpha \in (0, 1)$ , we aim to construct a conformal

interval  $\widehat{C}_C(\overline{B}) \subset \mathbb{R}$  for the cluster-level treatment effect such that

$$P\left\{\overline{Y}(1) - \overline{Y}(0) \in \widehat{C}_C(\overline{B})\right\} \geq 1 - \alpha, \quad (1)$$

where  $\overline{B} = (\overline{X}, R, N)$  is the cluster-level covariate information with  $\overline{X} = \frac{1}{N} \sum_{j=1}^{N_i} X_{\bullet,j}$  being the cluster-aggregate covariates. Equation (1) has the following interpretation: for any cluster sampled from  $\mathcal{P}^W$ , its cluster-level treatment effect,  $\overline{Y}(1) - \overline{Y}(0)$ , is guaranteed to be contained in  $\widehat{C}_C(\overline{B})$  with probability at least  $1 - \alpha$ , without requiring any asymptotic regimes. Therefore,  $\widehat{C}_C(\overline{B})$  naturally quantifies the cluster-level treatment effect by characterizing the most likely range of  $\overline{Y}(1) - \overline{Y}(0)$ . Distinct from the confidence interval  $\widehat{CI}_m$ ,  $\widehat{C}_C(\overline{B})$  is covariate-based and targets the random variable  $\overline{Y}(1) - \overline{Y}(0)$ . Then,  $\widehat{C}_C(\overline{B})$  essentially provides the  $(\alpha/2, 1 - \alpha/2)$ -quantile for the distribution of  $\overline{Y}(1) - \overline{Y}(0)$ . Of note, while the definition in (1) is directly motivated by the cluster-average estimand, the same framework can be directly applied to other cluster summaries such as cluster totals (Su and Ding, 2021).

Our target of inference also naturally extends to the construction of a conformal interval  $\widehat{C}_I(B)$  for the individual-level treatment effect such that

$$P\left\{Y(1) - Y(0) \in \widehat{C}_I(B)\right\} \geq 1 - \alpha. \quad (2)$$

Here,  $B = (X, R, N)$  is the individual-level covariate data, and  $\{Y(1), Y(0), X\}$  can represent any individual  $\{Y_{\bullet,j}(1), Y_{\bullet,j}(0), X_{\bullet,j}\}$  since they are identically distributed given  $N$  by Assumption 3. The interpretation of Equation (2) is similar to Equation (1): for any cluster sampled from  $\mathcal{P}^W$ , the individual-level treatment effect  $Y(1) - Y(0)$  is contained in  $\widehat{C}_I(B)$  with probability at least  $1 - \alpha$ . Similarly,  $\widehat{C}_I(B)$  characterizes the  $(\alpha/2, 1 - \alpha/2)$ -quantile of  $Y(1) - Y(0)$  and describes a personalized range. In contrast to the cluster-level treatment effect, which only pertains to independent cluster-level data, accomplishing the objectives in Equation (2) is more challenging due to the unknown intracluster correlations between observations inherent in CRTs.

Beyond (1) and (2), we further study conformal causal inference on pre-defined covariate

subgroups. Specifically, let  $\Omega_C$  and  $\Omega_I$  be arbitrary sets with positive measures in the support of  $\bar{B}$  and  $B$ , respectively. For example, if  $X_1$  represents age, we can define  $\Omega_C = \{\bar{B} : \bar{X}_1 \geq 70\}$  and  $\Omega_I = \{B : X_1 \geq 70\}$  to focus on the treatment effects on a specific age group. Given  $\Omega_C$  and  $\Omega_I$ , we aim to construct conformal intervals  $\tilde{C}_C(\bar{B})$  and  $\tilde{C}_I(B)$  such that

$$P\left\{\bar{Y}(1) - \bar{Y}(0) \in \tilde{C}_C(\bar{B}) \mid \bar{B} \in \Omega_C\right\} \geq 1 - \alpha, \quad (3)$$

$$P\left\{Y(1) - Y(0) \in \tilde{C}_I(B) \mid B \in \Omega_I\right\} \geq 1 - \alpha. \quad (4)$$

Equations (3) and (4) characterize “local coverage” that is distinct from “marginal coverage” characterized by Equations (1) and (2). With local coverage, the resulting conformal intervals provide more targeted information for specific sub-populations of interest (rather than the entire study population) and carry a finer resolution (in the same spirit of subgroup analyses). The marginal coverage definition is then viewed as a special case of local coverage by setting  $\Omega_C$  and  $\Omega_I$  to be the entire covariate support. Notably, local coverage differs from conditional coverage, where the probability measures are further conditioned on  $\bar{B}$  or  $B$ . Compared to local coverage, conditional coverage is a much stronger objective, whereas it has been proved impossible for continuous covariates (Lei and Wasserman, 2014).

Before moving to the technical development, we introduce some additional notation. Let  $\bar{Y} = A\bar{Y}(1) + (1 - A)\bar{Y}(0)$ ,  $I\{G\}$  denote the indicator function of event  $G$ ,  $\|\cdot\|_2$  is the  $\ell_2$  norm,  $\delta_s$  as a point mass at  $s$  in the Euclidean space, and  $\delta_{+\infty}$  is a point mass at infinity.

## 3 Conformal causal inference for cluster-level treatment effects

### 3.1 Inference for an observed cluster

For inferring cluster-level treatment effects, we aim to construct a conformal interval  $\tilde{C}_C$  given a test point  $\bar{B}_{\text{test}}$ , i.e., the cluster-aggregate covariates of a new cluster sampled from



the target population. We first consider a basic scenario, where we observe the complete information  $\bar{O}_{\text{test}} = (\bar{Y}_{\text{test}}, A_{\text{test}}, \bar{B}_{\text{test}})$  for the test point. In other words, this test point corresponds to an “observed cluster”, i.e., its current intervention  $A_{\text{test}}$  (likely not randomized, often  $A_{\text{test}} = 0$  and not included in the CRT) and current average outcome  $\bar{Y}(A_{\text{test}})$  are also recorded. Such additional data beyond  $\bar{B}_{\text{test}}$  will simplify the inference procedure since one of the two potential outcomes  $\{\bar{Y}_{\text{test}}(1), \bar{Y}_{\text{test}}(0)\}$  is directly observed, and the conformal causal inference only requires constructing the conformal interval for the unobserved average potential outcome.

Under this basic scenario, Algorithm 1 outlines the steps to compute the conformal interval  $\tilde{C}_C(\bar{O}_{\text{test}})$ . In the input phase, the prediction model  $f_a, a \in \{0, 1\}$  can be an arbitrary map from covariates to the outcome, e.g., a linear model, or random forest (Breiman, 2001). Different choices of  $f_a$  will not impact the coverage validity, but can result in conformal intervals with different lengths and thus affect precision. In addition, we need to specify the covariate subgroup of interest, e.g.,  $\Omega_C$  as the entire covariate support or  $\Omega_C = \{\bar{B}_i : \bar{X}_{i1} > 70, R_{i1} = \text{“Rural”}\}$  as a sub-population, and a level  $\alpha$ , e.g.,  $\alpha = 0.1$ . While a more restrictive  $\Omega_C$  can target a smaller sub-population, the resulting conformal interval may be wider due to fewer data points; we further discuss this trade-off in Section 7.

Given the input, we take two steps to construct the conformal interval. In the first step, we apply the split conformal prediction (Papadopoulos et al., 2002) to construct a conformal interval for one potential outcome  $\bar{Y}(a)$ , based on arm- $a$  data in the covariate subgroup characterized by  $\Omega_C$ . In split conformal prediction, the data are randomly partitioned into two halves, one used to train the prediction model  $f_a, a \in \{0, 1\}$ , (Steps 1.1-1.2) and the other used to construct the conformal interval (Steps 1.3-1.5). Compared to alternative methods such as full conformal prediction (Lei et al., 2018) and cross-validated conformal prediction (Barber et al., 2021), split conformal prediction uses random data partition to substantially reduce computational complexity. It therefore embraces practicality, despite its less efficient use of the data (Tibshirani et al., 2019). Given the model fit  $\hat{f}_a$ , Step 1.3 computes the non-conformity score  $s(b, y)$ , which is the absolute value of prediction error on calibration

---

**Algorithm 1** Computing the conformal interval  $\tilde{C}_C(\bar{O})$  for cluster-level treatment effects.

---

**Input:** Cluster-level data  $\{(\bar{Y}_i, A_i, \bar{B}_i) : i = 1, \dots, m\}$ , a test point  $\bar{O}_{\text{test}} = (\bar{Y}_{\text{test}}, A_{\text{test}}, \bar{B}_{\text{test}})$ , an arbitrary prediction model  $f_a(\bar{B})$  for  $\bar{Y}(a)$ ,  $a \in \{0, 1\}$ , a covariate subgroup of interest  $\Omega_C$ , and level  $\alpha$ .

**Step 1** (Constructing the conformal interval  $\tilde{C}_{C,a}(\bar{B})$  for  $\bar{Y}(a)$ .)

For  $a = 0, 1$ ,

1. Randomly split the arm- $a$  covariate subgroup data  $\{(\bar{Y}_i, \bar{B}_i) : i = 1, \dots, m, A_i = a, \bar{B}_i \in \Omega_C\}$  into a training fold  $\mathcal{O}_{tr}(a)$  and a calibration fold  $\mathcal{O}_{ca}(a)$  with index set  $\mathcal{I}_{ca}(a)$ .

2. Train the prediction model  $f_a(\bar{B})$  using the training fold  $\mathcal{O}_{tr}(a)$ , and obtain the estimated model  $\hat{f}_a(\bar{B})$ .

3. For each  $i \in \mathcal{I}_{ca}(a)$ , compute the non-conformity score  $s(\bar{B}_i, \bar{Y}_i) = |\bar{Y}_i - \hat{f}_a(\bar{B}_i)|$ .

4. Compute the  $1 - \alpha$  quantile  $\hat{q}_{1-\alpha}(a)$  of the distribution

$$\hat{F} = \frac{1}{|\mathcal{I}_{ca}(a)| + 1} \left\{ \sum_{i \in \mathcal{I}_{ca}(a)} \delta_{s(\bar{B}_i, \bar{Y}_i)} + \delta_{+\infty} \right\}.$$

5. Obtain  $\tilde{C}_{C,a}(\bar{B}) = \{y \in \mathbb{R} : |y - \hat{f}_a(\bar{B})| \leq \hat{q}_{1-\alpha}(a)\}$ .

**Step 2** (Constructing the conformal interval  $\tilde{C}_C(\bar{O})$  for  $\bar{Y}(1) - \bar{Y}(0)$ .)

If  $A_{\text{test}} = 1$ , then set  $\tilde{C}_C(\bar{O}_{\text{test}}) = \bar{Y}_{\text{test}} - \tilde{C}_{C,0}(\bar{B}_{\text{test}})$ ;

if  $A_{\text{test}} = 0$ , then set  $\tilde{C}_C(\bar{O}_{\text{test}}) = \tilde{C}_{C,1}(\bar{B}_{\text{test}}) - \bar{Y}_{\text{test}}$ .

**Output:**  $\tilde{C}_C(\bar{O}_{\text{test}})$ .

---

data. Intuitively, a large non-conformity score indicates an abnormal data point (i.e., it does not “conform”) with respect to  $\hat{f}_a$ . In Step 1.5, we construct  $\tilde{C}_{C,a}(\bar{B})$  by excluding  $y$  with a large non-conformity score  $s(\bar{B}, y)$ . The threshold,  $\hat{q}_{1-\alpha}$ , as the exclusion criterion is defined as the  $(1 - \alpha)$ -quantile of the empirical distribution on the non-conformity score (plus a point mass at infinity). The underlying idea of this threshold comes from a neat observation: for exchangeable variables  $(V_1, \dots, V_n, V_{n+1})$ ,  $V_{n+1}$  is smaller than the  $(1 - \alpha)$ -quantile of their empirical distribution with probability at least  $1 - \alpha$ . Following this logic, the constructed  $\tilde{C}_{C,a}(\bar{B})$  has probability no less than  $1 - \alpha$  to contain  $\bar{Y}(a)$ . With  $\tilde{C}_{C,a}(\bar{B})$  obtained from Step 1, we proceed to Step 2, where  $\tilde{C}_C(\bar{O}_{\text{test}}) = (-1)^{A_{\text{test}}+1} \{\bar{Y}_{\text{test}} - \tilde{C}_{C,1-A_{\text{test}}}(\bar{B}_{\text{test}})\}$  is the output. In other words, the final conformal interval is a contrast between the observed potential outcome and the interval constructed for the unobserved potential outcome.

Theorem 1 proves that  $\tilde{C}_C(\bar{O}_{\text{test}})$  achieves finite-sample coverage guarantee for the cluster-level treatment effect, without requiring Assumption 3 on within-cluster exchangeability.

**Theorem 1.** *Under Assumptions 1-2 and assuming that  $\bar{O}_{\text{test}} = (\bar{Y}_{\text{test}}, A_{\text{test}}, \bar{B}_{\text{test}})$  is an independent sample from the distribution  $\mathcal{P}^{\bar{O}}$  induced by  $\mathcal{P}^W \times \tilde{\mathcal{P}}^{A|W}$  and  $\bar{Y}_{\text{test}} = A_{\text{test}}\bar{Y}_{\text{test}}(1) + (1 - A_{\text{test}})\bar{Y}_{\text{test}}(0)$ , where  $\tilde{\mathcal{P}}^{A|W}$  is an arbitrary unknown distribution for  $A_{\text{test}}$ . Then, the conformal interval  $\tilde{C}_C(\bar{O}_{\text{test}})$  output by Algorithm 1 satisfies*

$$P\left\{\bar{Y}_{\text{test}}(1) - \bar{Y}_{\text{test}}(0) \in \tilde{C}_C(\bar{O}_{\text{test}}) \mid \bar{B}_{\text{test}} \in \Omega_C\right\} \geq 1 - 2\alpha \quad (5)$$

for any set  $\Omega_C$  in the support of  $\bar{B}_{\text{test}}$  with a positive measure.

Theorem 1 is a direct generalization of the conformal prediction theory to conformal causal inference on covariate subgroups. Since we observe  $\bar{Y}_{\text{test}}$  and  $A_{\text{test}}$ , the valid coverage for the treatment effect is straightforward once we achieve valid coverage for the potential outcome. However, since we need to account for arbitrary distribution shift on  $A_{\text{test}}$  from  $\mathcal{P}^A$  to  $\tilde{\mathcal{P}}^{A|W}$ , the non-coverage rate  $\alpha$  is doubled in Equation (5) by applying the union bound. If  $\tilde{\mathcal{P}}^{A|W}$  is independent of  $W$  (e.g.,  $P(A_{\text{test}} = 1) = 0$  when studying a new intervention or  $A_{\text{test}}$  is randomized), then the coverage probability achieves  $1 - \alpha$  in Equation (5). For local coverage, we consider a simple yet effective approach that only clusters with  $\bar{B}_i \in \Omega_C$  are included. Technically, it changes the covariate distribution but not the outcome distribution given covariates, thereby not changing the coverage result. Recently, Hore and Barber (2023) proposed an approach to construct the conformal interval that is independent of  $\Omega_C$ , whereas this uniformity property can lead to poor coverage (e.g., zero) in many covariate subgroups and, more importantly, discrete covariates cannot be directly handled by their localization kernels. Furthermore, it is worth mentioning two important special cases of Theorem 1. When  $P(\bar{B} \in \Omega_C) = 1$ , Equation (5) implies marginal coverage in Equation (1). Setting  $N_i = 1$ , Theorem 1 also applies to conformal causal inference for individually randomized trials.

In practice, how to choose  $\alpha$  and the size of the training fold depends on the number of

clusters  $m$ . To obtain a non-trivial conformal interval such that  $\tilde{C}_C(\overline{O}_{\text{test}}) \neq \mathbb{R}$ , the definition of  $\hat{q}_{1-\alpha}(a)$  requires that  $\alpha \geq |\mathcal{I}_{ca}(a)|^{-1}$ . For example, if we set  $\alpha = 0.1$ , then the calibration fold for each arm should contain at least 10 clusters, and the rest  $m - 20$  clusters can be used as the training fold. For stability of model fitting, we recommend using at least 20 clusters for training, while fewer clusters are also acceptable if parsimonious models such as linear regression are used. When the number of clusters is small, e.g.,  $m = 20$ , Algorithm 1 based on split conformal prediction cannot construct non-trivial conformal intervals with 90% coverage probability. However, this goal is achievable with full conformal prediction or Jackknife+, but demands a substantially higher computation cost (Barber et al., 2021).

### 3.2 Inference based on cluster-level covariates

When the target of inference concerns a new cluster that only has covariate information  $\overline{B}_{\text{test}}$  (e.g., a cluster having not taken either treatment or control studied in the current CRT), a direct approach based on Algorithm 1 is to combine  $\tilde{C}_{C,1}$  and  $\tilde{C}_{C,0}$ , for which Corollary 1 characterizes its local coverage property.

**Corollary 1.** *Under Assumptions 1-2 and assuming that  $(\overline{Y}_{\text{test}}(1), \overline{Y}_{\text{test}}(0), \overline{B}_{\text{test}})$  is an independent sample from the distribution  $\mathcal{P}^W$ . Then,  $\tilde{C}_{C,1}(\overline{B}_{\text{test}})$  and  $\tilde{C}_{C,0}(\overline{B}_{\text{test}})$  output by Algorithm 1 satisfy*

$$P\left\{\overline{Y}_{\text{test}}(1) - \overline{Y}_{\text{test}}(0) \in \tilde{C}_{C,1}(\overline{B}_{\text{test}}) - \tilde{C}_{C,0}(\overline{B}_{\text{test}}) \mid \overline{B}_{\text{test}} \in \Omega_C\right\} \geq 1 - \alpha \quad (6)$$

for any set  $\Omega_C$  in the support of  $\overline{B}_{\text{test}}$  with a positive measure.

Compared to Equation (5), Equation (6) provides a stronger coverage probability  $1 - \alpha$ , but the length of the conformal interval can be approximately doubled since we no longer observe  $\overline{Y}_{\text{test}}$  and  $A_{\text{test}}$ . As a result, the conformal interval is based on  $\overline{B}_{\text{test}}$  tends to be less informative than  $\tilde{C}_C(\overline{O}_{\text{test}})$ , a natural result of less observed information.

Beyond this direct approach, Lei and Candès (2021) provided a more flexible nested approach to construct  $\tilde{C}_C(\overline{B}_{\text{test}})$ . This method first computes  $\overline{C}_i$ , the  $(1 - \alpha)$ -conformal

interval for  $\bar{Y}(1) - \bar{Y}(0)$ , using  $\tilde{C}_{C,a}$  from Algorithm 1, and then run split conformal prediction again on  $(\bar{C}_i, \bar{B}_i)$  with level  $\gamma$  and prediction models  $(m^L, m^R)$ . Since we run split conformal prediction twice, the resulting conformal interval  $\tilde{C}_C(\bar{B}_{\text{test}})$  has non-coverage probability up to  $\alpha + \gamma$ . For completeness, we provide the detailed algorithm and its theoretical guarantee in the Supporting Information. Finally, we remark that the nested approach becomes similar to the direct approach with  $\gamma$  set equal to  $\alpha$ . In practice, both the direct and nested approaches tend to be conservative since  $\{\bar{Y}(1), \bar{Y}(0)\}$  are not observed, but the nested approach can alleviate conservativeness by specifying a larger  $\gamma$  and trading the theoretical guarantee for better empirical performance.

## 4 Conformal causal inference for individual-level treatment effects

So far, we have extended conformal causal inference for the cluster-level treatment effects by treating cluster-level data as independent units. However, for individual-level treatment effects, the existing theory for conformal inference cannot be directly applied since the individual-level data are clustered. This feature presents apparent challenges in obtaining conformal intervals with either marginal or local coverage guarantees. Lee et al. (2023) developed recent results for conformal inference with hierarchical data, focusing on the setting where individuals in the same cluster are conditionally independent. We consider this setting overly restrictive because it rules out any unmeasured source of within-cluster correlations and is not even compatible with a random-intercept linear mixed model. Below, we provide the algorithm and theory for conformal causal inference on the individual-level treatment effect estimand under a more general exchangeability setup characterized by Assumption 3.

### 4.1 Inference for an observed individual

We first consider a basic setting, where the test point has the complete information  $O_{\text{test}} = (Y_{\text{test}}, A_{\text{test}}, B_{\text{test}})$ . This setting corresponds to an observed individual in an observed cluster

of interest, whose current treatment  $A_{\text{test}}$  may not be randomized. Similar to our development in Section 3.1, we only need to construct the conformal interval for the unobserved potential outcome, leading to higher chances of narrower and more informative conformal intervals.

In Algorithm 2, we show how to construct the conformal interval  $\tilde{C}_I(O)$  for  $Y(1) - Y(0)$ . Compared to Algorithm 1, the major difference is in Step 1.4: the new empirical distribution function  $\hat{F}$  only involves individuals meeting the criteria  $B_{ij} \in \Omega_I$ , and each individual is further weighted by  $\left(\sum_{j=1}^{N_i} I\{B_{ij} \in \Omega_I\}\right)^{-1}$ ; all other steps remain similar but now apply to the individual data (rather than cluster aggregate). Since we target inference on specific covariate subgroups characterized by  $\Omega_I$  (which again can be the entire support), we prove a Lemma in the Supporting Information to show that Assumptions 1-3 holds when restricting to any subgroup  $\Omega_I$  with a positive measure. This is a critical step to preserve the exchangeable structure within clusters and develop our theoretical results. Furthermore, the clustered data structure is handled by inverse weighting: with these weights, point masses within a cluster are symmetric, and the cluster-average point masses are also symmetric across clusters. Although the technical details are more complex and explained in the Supporting Information, intuitively, the multilevel symmetry of  $\hat{F}$  links the test data and calibration data as in the setting of exchangeable data, based on which we can derive finite-sample robustness. The theoretical guarantee of the resulting conformal interval is formally stated in Theorem 2.

**Theorem 2.** *Under Assumptions 1-3 and assuming that  $O_{\text{test}} = (Y_{\text{test}}, A_{\text{test}}, B_{\text{test}})$  is an arbitrary individual in a new cluster independently sampled from  $\mathcal{P}^W \times \tilde{\mathcal{P}}^{A|W}$  with  $Y_{\text{test}} = A_{\text{test}}Y_{\text{test}}(1) + (1 - A_{\text{test}})Y_{\text{test}}(0)$ , where  $\tilde{\mathcal{P}}^{A|W}$  is an arbitrary unknown distribution for  $A_{\text{test}}$ . Then, the  $\tilde{C}_I(O_{\text{test}})$  output by Algorithm 1 satisfies*

$$P\left\{Y_{\text{test}}(1) - Y_{\text{test}}(0) \in \tilde{C}_I(O_{\text{test}}) \mid B_{\text{test}} \in \Omega_I\right\} \geq 1 - 2\alpha \quad (7)$$

for any set  $\Omega_I$  in the support of  $B_{\text{test}}$  with a positive measure.

---

**Algorithm 2** Computing the conformal interval  $\tilde{C}_I(O)$  for individual-level treatment effects.

**Input:** Individual-level data  $\{(Y_{ij}, A_i, B_{ij}) : i = 1, \dots, m; j = 1, \dots, N_i\}$ , a test point  $O_{\text{test}} = (Y_{\text{test}}, A_{\text{test}}, B_{\text{test}})$ , a prediction model  $f_a(B)$  for  $Y(a)$ ,  $a \in \{0, 1\}$ , a covariate subgroup of interest  $\Omega_I$ , and level  $\alpha$ .

**Step 1** (Constructing the conformal interval  $\tilde{C}_{I,a}(B)$  for  $Y(a)$ .)

For  $a = 0, 1$ ,

1. Randomly split the arm- $a$  covariate subgroup data  $\{(Y_{ij}, A_i, B_{ij}) : i = 1, \dots, m; j = 1, \dots, N_i; A_i = a; B_{ij} \in \Omega_I\}$  into a training fold  $\mathcal{O}_{tr}(a)$  and a calibration fold  $\mathcal{O}_{ca}(a)$  with index set  $\mathcal{I}_{ca}(a)$ .

2. Train the prediction model  $f_a(B)$  using the training fold  $\mathcal{O}_{tr}(a)$ , and obtain the estimated model  $\hat{f}_a(B)$ .

3. For each  $(i, j) \in \mathcal{I}_{ca}(a)$ , compute the non-conformity score  $s(B_{ij}, Y_{ij}) = |Y_{ij} - \hat{f}_a(B_{ij})|$ .

4. Compute the  $1 - \alpha$  quantile  $\hat{q}_{1-\alpha}(a)$  of the distribution

$$\hat{F} = \frac{1}{|\mathcal{I}_{ca}(a)| + 1} \left\{ \sum_{i \in \mathcal{I}_{ca}(a)} \frac{1}{\sum_{j=1}^{N_i} I\{B_{ij} \in \Omega_I\}} \sum_{j=1}^{N_i} I\{B_{ij} \in \Omega_I\} \delta_{s(B_{ij}, Y_{ij})} + \delta_{+\infty} \right\}.$$

5. Obtain  $\tilde{C}_{I,a}(B) = \{y \in \mathbb{R} : |y - \hat{f}_a(B)| \leq \hat{q}_{1-\alpha}(a)\}$ .

**Step 2** (Constructing the conformal interval  $\tilde{C}_I(O)$  for  $Y(1) - Y(0)$ .)

If  $A_{\text{test}} = 1$ , then set  $\tilde{C}_I(O_{\text{test}}) = Y_{\text{test}} - \tilde{C}_{I,0}(B_{\text{test}})$ ;

if  $A_{\text{test}} = 0$ , then set  $\tilde{C}_I(O_{\text{test}}) = \tilde{C}_{I,1}(B_{\text{test}}) - Y_{\text{test}}$ .

**Output:**  $\tilde{C}_I(O_{\text{test}})$ .

---

Theorem 2 is the counterpart of Theorem 1 characterizing the local or marginal coverage property for individual-level treatment effects, depending on the choice of  $\Omega_I$ . Due to the distribution shift on  $A_{\text{test}}$ , the coverage probability is  $1 - 2\alpha$  instead of  $1 - \alpha$ , while the latter can be achieved if  $\tilde{\mathcal{P}}^{A|W}$  is independent of  $W$  (e.g.,  $A_{\text{test}} \equiv 0$ ). When each cluster only has one individual, Algorithm 1 and Algorithm 2 coincide, and their resulting coverage guarantees also become identical.

From the perspective of implementation, conformal causal inference for individual-level treatment effects is advantageous in model training over that for cluster-level treatment effects. As a concrete context, given 10 clusters, learning the cluster-level model for  $\bar{Y}(1) - \bar{Y}(0)$  includes 10 data points as its effective sample size, which may potentially lead to overfitting with a handful of covariates. In contrast, the individual-level model for  $Y(1) -$

$Y(0)$  often has a larger effective sample size for training, e.g., 300 data points given 30 individuals per cluster. Since the within-cluster correlation is usually small (Campbell et al., 2005), the increased effective sample size in the training data can substantially improve the numerical stability. As a result, conformal causal inference for individual-level treatment effects could be more informative in CRTs with a small  $m$  compared to that for cluster-level treatment effects. As we demonstrate in the ensuing simulations, with  $m = 30$  clusters, we are able to perform conformal subgroup analysis for the individual-level treatment effect but not the cluster-level treatment effect.

In terms of the length of conformal intervals,  $\tilde{C}_C(\bar{B}_{\text{test}})$  tends to be more informative than  $\tilde{C}_I(B_{\text{test}})$  given a sufficient number of clusters. This is because  $\bar{Y}(1) - \bar{Y}(0)$  often has smaller variance than  $Y(1) - Y(0)$ , especially if  $N_i$  is large. As a result,  $\tilde{C}_C(\bar{B}_{\text{test}})$  is more likely to exclude zero than  $\tilde{C}_I(B_{\text{test}})$  given the same treatment effect size. In practice, choosing between the two types of inferential targets requires a case-by-case evaluation. Although the scientific question should drive the target of inference, from a statistical perspective, conformal causal inference for the cluster-level treatment effects with  $\alpha = 0.1$  is typically more informative and efficient when  $m$  is large, e.g.,  $m \geq 80$ . Given a small to moderate number of clusters, the individual-level treatment effects are preferable, and  $\alpha$  can be adjusted accordingly to meet the practical needs.

## 4.2 Inference based on individual-level covariates

When the test point only contains individual-level covariates  $B_{\text{test}}$ , we follow the same strategy as in Section 3.2 to construct conformal intervals. Corollary 2 characterizes the local coverage property of the direct approach as an application of Theorem 2.

**Corollary 2.** *Under Assumptions 1-3 and assuming that  $(Y_{\text{test}}(1), Y_{\text{test}}(0), B_{\text{test}})$  is an arbitrary individual from a new cluster independently sampled from  $\mathcal{P}^W$ . Then  $\tilde{C}_{I,1}(B_{\text{test}})$  and  $\tilde{C}_{I,0}(B_{\text{test}})$  output by Algorithm 2 satisfy*

$$P\left\{Y_{\text{test}}(1) - Y_{\text{test}}(0) \in \tilde{C}_{I,1}(B_{\text{test}}) - \tilde{C}_{I,0}(B_{\text{test}}) \mid B_{\text{test}} \in \Omega_I\right\} \geq 1 - \alpha \quad (8)$$



for any set  $\Omega_I$  in the support of  $B_{\text{test}}$  with a positive measure.

In parallel to Corollary 1, Corollary 2 establishes the coverage guarantee on conformal intervals for the individual-level treatment effect based on covariates. In addition, the resulting conformal interval enjoys the same benefit of stability and small-sample compatibility as discussed in Section 4.1. In addition to the direct approach, we provided the nested approach with  $1 - \alpha - \gamma$  coverage guarantee in the Supporting Information.

## 5 Simulations

Through a simulation study, we aim to demonstrate our algorithms and verify our finite-sample theoretical results for both cluster-level and individual-level treatment effects. We consider the combination of the following settings: CRTs with a large ( $m = 100$ ) versus small ( $m = 30$ ) number of clusters, and full-data analysis versus covariate subgroup analysis.

### 5.1 Simulation design

For  $i = 1, \dots, m$ , we independently generate the cluster size  $N_i \sim \mathcal{U}([10, 50])$  and two cluster-level covariates  $R_{i1}|N_i \sim \mathcal{N}(N_i/10, 1)$ ,  $R_{i2}|(N_i, R_{i1}) \sim \mathcal{B}\{(1 + e^{-R_{i1}/2})^{-1}\}$ , where  $\mathcal{U}, \mathcal{N}, \mathcal{B}$  represent the uniform, normal, and Bernoulli distribution, respectively. For each individual  $j = 1, \dots, N_i$ , we independently generate covariates  $X_{ij1}|(N_i, R_{i1}, R_{i2}) \sim \mathcal{B}(0.3 + 0.4R_{i2})$  and  $X_{ij2} = (2I\{R_{i1} > 0\} - 1)\bar{X}_{i1} + \mathcal{N}(0, 1)$ , and potential outcomes

$$\begin{aligned} Y_{ij}(0) &= \sin(R_{i1})(2R_{i2} - 1) + |X_{ij1}X_{ij2}| + \gamma_i + \varepsilon_{ij} \\ Y_{ij}(1) &= \sin(R_{i1})(2R_{i2} - 1) + |X_{ij1}X_{ij2}| + N_i/50 + \varepsilon_{ij}, \end{aligned}$$

where  $\gamma_i \sim \mathcal{N}(0, 0.5^2)$  is the random intercept and  $\varepsilon_{ij} \sim \mathcal{N}(0, 1)$  is the random noise. Then we independently generate the treatment indicator  $A_i \sim \mathcal{B}(0.5)$ , and obtain  $Y_{ij} = A_i Y_{ij}(1) + (1 - A_i) Y_{ij}(0)$ . The simulated observed data are  $\{(Y_{ij}, A_i, X_{ij1}, X_{ij2}, R_{i1}, R_{i2}) : i = 1, \dots, m, j = 1, \dots, N_i\}_{i=1}^m$ . In addition, we generate 1,000 new clusters as the test data, following the

same data-generating distribution. We repeat the above procedure to generate 1,000 data replicates for evaluation of the conformal interval estimators.

For each simulated data set, we first construct the conformal interval for the cluster-average treatment effect. Given complete test data (with treatment and outcomes), we run Algorithm 1, and refer to this approach as “O”. Given cluster-level covariates only, we refer to the direct approach as “B-direct” and the nested approach as “B-nested”. For covariate subgroup analysis, we consider  $\Omega_C = \{\bar{B}_i : R_{i1} \geq 2, R_{i2} = 1\}$ , which contains 60% of all clusters. For inferring the individual-average treatment effect, we adopt the same names “O”, “B-direct”, “B-nested” to refer to the output of Algorithm 2, the direct approach and the nested approach, and the covariate subgroup is defined as  $\Omega_I = \{B_{ij} : |X_{ij2}| < 0.5\}$ , which includes 30% of all individuals. For each method, the training model uses an ensemble learner of linear regression and random forest through the SuperLearner package (van der Laan et al., 2007) in the R software. We consider two metrics of performance based on the test data: the probability that the conformal interval contains the true treatment effect, and the average length of the conformal interval. When  $m = 100$ , we set  $\alpha = 0.1$ , while we consider both  $\alpha = 0.1$  and  $\alpha = 0.2$  given  $m = 30$ . For the nested approach, we set  $\gamma = 0.5$  to improve the informativeness of the resulting conformal interval.

## 5.2 Simulation results

Figure 1 summarizes the simulation results for the marginal and local cluster-level treatment effects given  $m = 100$ . In Figure 1, the upper panels show that all three methods achieve the target 90% coverage probability, thereby confirming our theoretical results. Comparing the three methods, the “O” method has a coverage probability close to 0.9, whereas the “B-direct” method is the most conservative one (coverage probability near 1). This difference can be explained by the lower panels, where the “B-direct” method yields wider conformal intervals, whose length nearly doubles the oracle length. In contrast, due to leveraging the complete information in the test data, the “O” method achieves the near-optimal length of the conformal interval. The performance of the “B-nested” method lies between the other

two since we set a loose parameter  $\gamma = 0.5$ . If we use  $\gamma = 0.1$  instead, it will perform similarly to the “B-direct” method as demonstrated in [Lei and Candès \(2021\)](#) for non-clustered data. Comparing marginal versus local treatment effects, the coverage probability and length of conformal intervals are both similar, while the results for the local treatment effect are slightly less stable with fewer data points. In the Supporting Information, we reproduce [Figure 1](#) with  $m = 500$ , where the span of the boxplot substantially decreases and the “O” method is nearly optimal under both metrics, confirming the large-sample stability.

[Figure 2](#) presents the simulation results for the marginal and local individual-level treatment effects given  $m = 100$ . All three methods reach the target coverage probability, and their comparisons are similar to [Figure 1](#). However, the conformal intervals for the individual-level treatment effect are more stable than the cluster-level treatment effect, as reflected by shorter spans of the boxplot, but have wider lengths due to the increased variance in treatment effects. The large sample stability is similarly confirmed by reproducing [Figure 2](#) with  $m = 500$  in the Supporting Information.

When  $m = 30$ , we provide the simulation results in [Table 1](#). Due to limited clusters, we do not implement the “B-nested” method (which requires two sample splittings) or perform the covariate-subgroup analysis for the cluster-level treatment effect (which drops 40% of all clusters). For the remaining scenarios, the “O” and “B-direct” methods can still achieve the target coverage probability, confirming their finite-sample validity. However, they become more conservative compared to  $m = 100$ , as reflected by the increased length of intervals. This is expected given limited clusters used in model training and quantile estimation. An ad-hoc solution is to consider an 80% coverage probability, in which case the resulting conformal intervals have a reduced length and are likely more informative. Finally, it is worth highlighting that, even with few clusters, we are able to perform subgroup analysis for the individual-level treatment effect, and its empirical performance is similar to the marginal analysis that uses all data. This observation confirms the statistical benefit of conformal causal inference for individual-level treatment effects in small CRTs.

In the Supporting Information, we provide additional simulations to evaluate the benefit

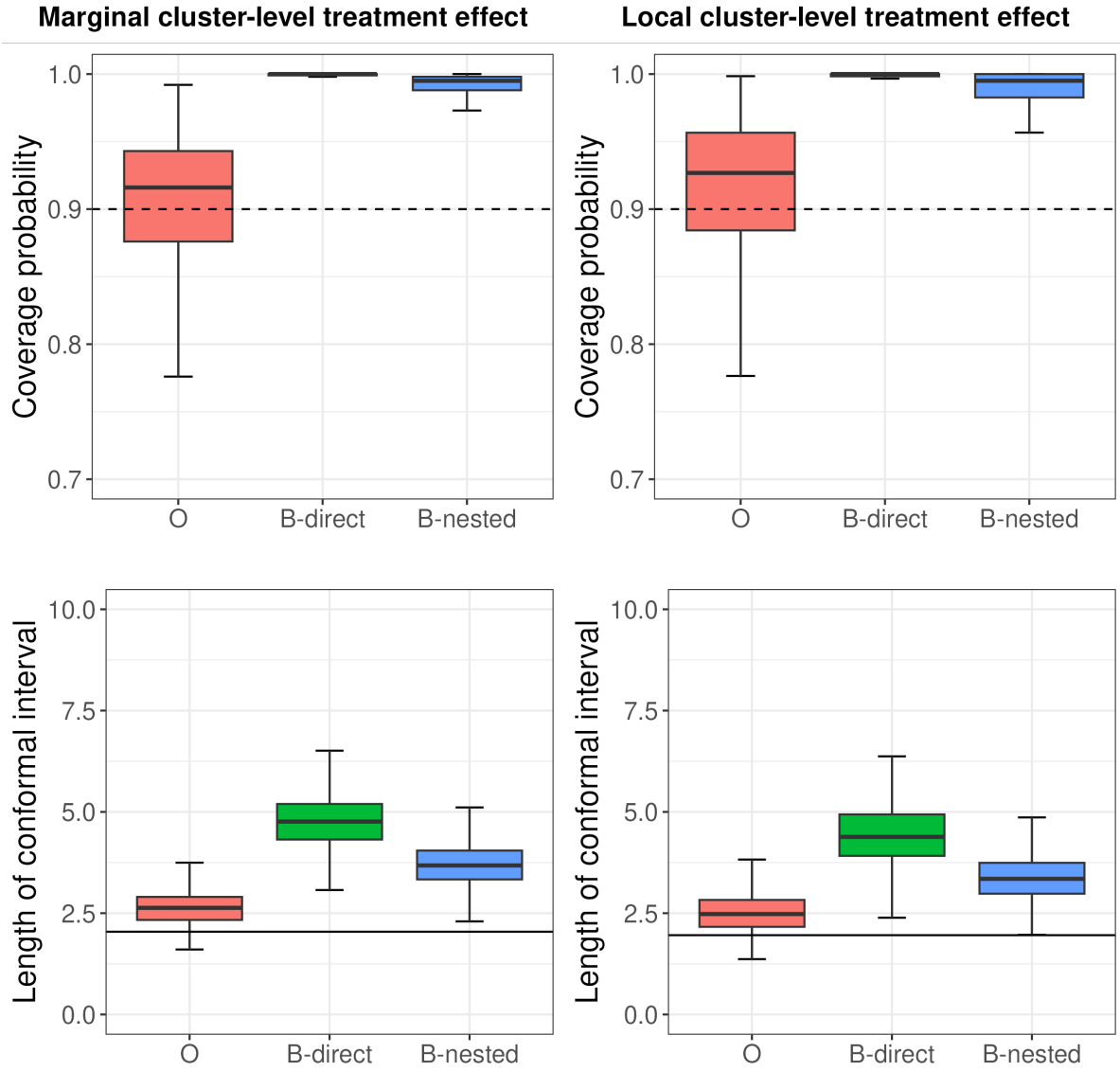


Figure 1: Simulation results (boxplot) for the marginal (left column) and local (right column, conditioning on  $\{R_{i1} \geq 2, R_{i2} = 1\}$ ) cluster-level treatment effects with  $m = 100$ . In the upper panels, the dashed line is the target 90% coverage probability. In the lower panels, the solid line is the oracle length of conformal intervals, computed as the average length between the  $(\alpha/2, 1 - \alpha/2)$ -quantiles of  $\bar{Y}(1) - \bar{Y}(0)$  among test data.

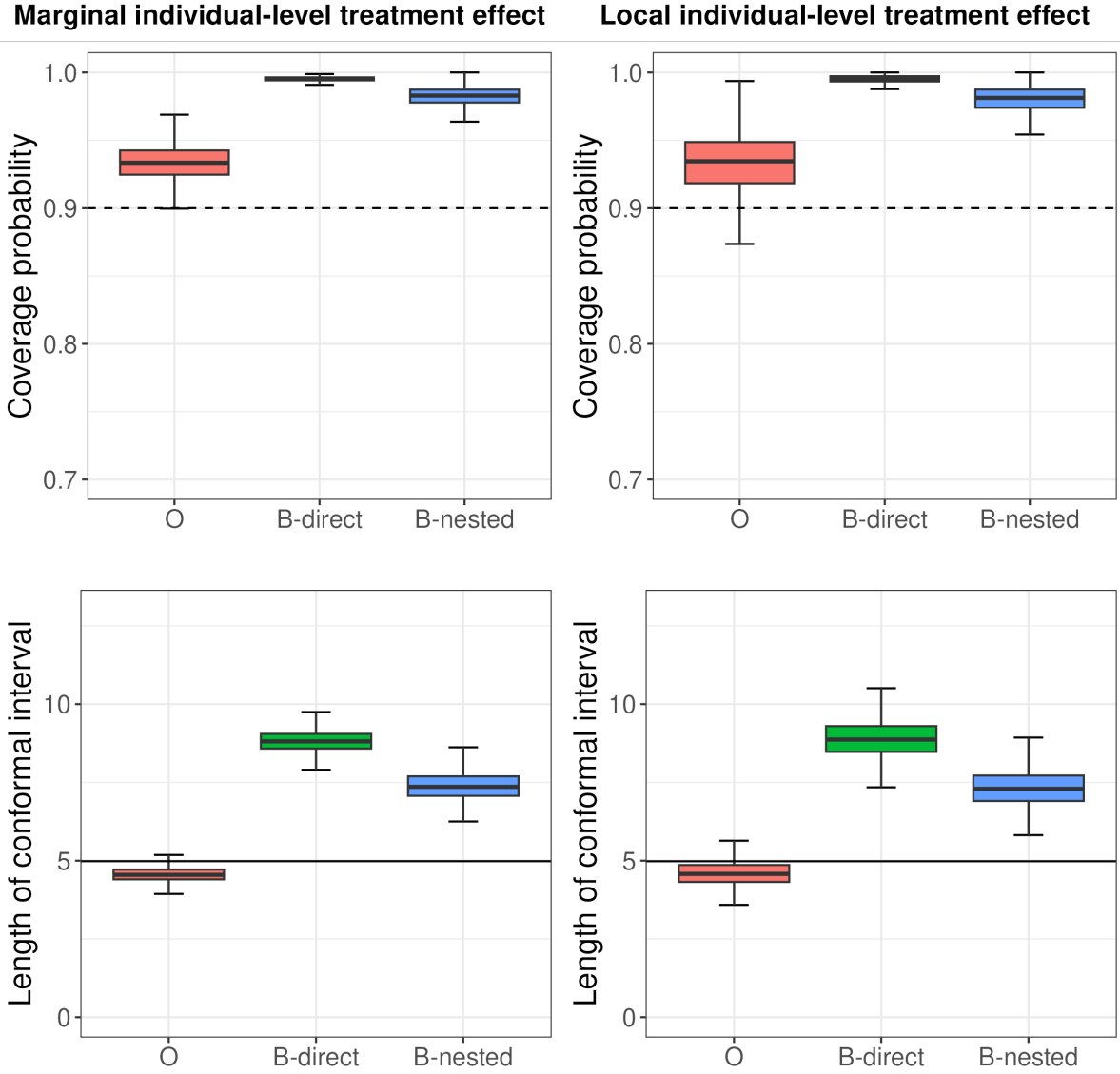


Figure 2: Simulation results (boxplot) for the marginal (left column) and local (right column, conditioning on  $\{|X_{ij2}| < 0.5\}$ ) individual-level treatment effects with  $m = 100$ . In the upper panels, the dashed line is the target 90% coverage probability. In the lower panels, the solid line is the oracle length of conformal intervals, computed as the average length between the  $(\alpha/2, 1 - \alpha/2)$ -quantiles of  $Y(1) - Y(0)$  among test data.

Table 1: Summary of simulation results for 80% and 90% conformal intervals given  $m = 30$  clusters. For both coverage probability and length of intervals, we report their averages and standard errors. The local treatment effect is conditioned on  $|X_{ij1}| < 0.5$ .

Treatment effects	Methods	$\alpha = 0.2$		$\alpha = 0.1$	
		Coverage probability	Length of intervals	Coverage probability	Length of intervals
Marginal cluster-level	O	0.816(0.094)	3.119(1.465)	0.912(0.072)	4.211(2.230)
	B-direct	0.998(0.008)	5.891(2.833)	1.000(0.002)	7.970(4.447)
Marginal individual-level	O	0.868(0.035)	4.311(0.489)	0.977(0.014)	6.637(0.794)
	B-direct	0.989(0.007)	8.345(0.768)	1.000(0.000)	12.905(1.232)
Local individual-level	O	0.870(0.048)	4.337(0.675)	0.977(0.021)	6.933(1.260)
	B-direct	0.988(0.009)	8.398(1.138)	1.000(0.000)	13.542(2.114)

of machine learning in fitting the prediction model. Specifically, we repeat our simulation study for  $m = 30$  with only linear regression as  $f_a$  (in contrast to the ensemble method with linear regression and random forest). We find that, by including random forest, the coverage probability has negligible differences, but the length of intervals is reduced by 8.2-46.5% across scenarios. This example further demonstrates that our method is able to leverage the power of machine learning to improve accuracy.

## 6 Data example with the PPACT cluster randomized trial

The Pain Program for Active Coping and Training study (PPACT) is a CRT evaluating the effect of a care-based cognitive behavioral therapy intervention for treating long-term opioid users with chronic pain (DeBar et al., 2022). The study equally randomized 106 primary care providers (clusters) to receive the intervention or usual care, with 1-10 participants in each cluster. We focus on the primary outcome, the PEGS (pain intensity and interference with enjoyment of life, general activity, and sleep) score at 12 months, a continuous measure of pain scale ranging from 1 to 10. For more accurate conformal causal inference, we adjust for 13 individual-level baseline variables, including the baseline PEGS score, age, gender, disability, smoking status, body mass index, alcohol abuse, drug abuse, comorbidity,

depression, number of pain types, average morphine dose, and heavy opioid usage.

Since the underlying truth of PPACT is unknown, we randomly sample 20 clusters as the test data and use the remaining 86 clusters to construct the conformal intervals. To account for the uncertainty introduced by random sampling, we repeat this procedure 100 times and report the average and standard error for two performance metrics: length of intervals and fraction of negatives. Here, the fraction of negatives defines the proportion of conformal intervals that are subsets of  $(-\infty, 0)$  among the test data. Since negative values are in the direction of treatment benefits, this metric reveals how many clusters/individuals are associated with beneficial treatment effects with probability  $1 - \alpha$ . Because the test data have the complete information, we directly run the ‘‘O’’ method, i.e., Algorithm 1 and Algorithm 2, with  $f_a$  set as the ensemble method of linear regression and random forest.

Table 2 summarizes the results for the marginal treatment effects setting  $\alpha \in \{0.1, 0.2, 0.3, 0.4\}$ . As  $\alpha$  increases, the length of intervals decreases, and the fraction of negative becomes larger. Since the treatment effect is small (relative to the variability of treatment effects, DeBar et al., 2022), only a small to moderate proportion of the population has negative conformal intervals. In practice, these negative conformal intervals can be informative for new patients with similar baseline characteristics.

Table 2: Summary results of data application for marginal treatment effects. For both the length of intervals and the fraction of negatives, we present the average and standard error over 100 runs.

Coverage probability	Marginal cluster-level treatment effect		Marginal individual-level treatment effect	
	Length of intervals	Fraction of negatives	Length of intervals	Fraction of negatives
90%	4.056(0.557)	0.089(0.069)	6.908(0.590)	0.055(0.026)
80%	2.874(0.412)	0.173(0.092)	4.800(0.345)	0.132(0.044)
70%	2.233(0.313)	0.238(0.104)	3.811(0.220)	0.199(0.052)
60%	1.799(0.255)	0.304(0.117)	3.108(0.189)	0.257(0.055)

In addition to the marginal analysis, we performed subgroup analyses on individuals with severe baseline pain (baseline PEGS score equal to or larger than 7, 40% participants) and moderate baseline pain (baseline PEGS score between 4 and 7, 50% participants). We summarize the results in Table 3, which shows no difference in the length of intervals or the

fraction of negatives between the two subgroups. Overall, these analyses indicate treatment benefits for a small subset of the clusters/individuals, which drive the overall treatment effect signal provided in previous analyses (DeBar et al., 2022; Wang et al., 2023).

Table 3: Summary results of data application for individual-level treatment effects on covariate subgroups. For both the length of intervals and the fraction of negatives, we present the average and standard error over 100 runs.

Coverage probability	Subgroup: severe baseline pain		Subgroup: moderate baseline pain	
	Length of intervals	Fraction of negatives	Length of intervals	Fraction of negatives
90%	6.538(0.571)	0.072(0.042)	6.508(0.538)	0.076(0.042)
80%	4.982(0.465)	0.120(0.051)	4.928(0.417)	0.132(0.053)
70%	3.935(0.353)	0.180(0.064)	3.960(0.349)	0.185(0.068)
60%	3.180(0.262)	0.243(0.067)	3.221(0.296)	0.241(0.079)

## 7 Discussion

In this work, we contributed a novel conformal causal inference framework for finite-sample model-robust inference in CRTs. Distinct from the classical framework that focuses on average treatment effects and often relies on the asymptotic theory, conformal causal inference yields covariate-based (thus personalized) intervals and is robust to arbitrary working model misspecification without appealing to asymptotic regimes. These new features address the limitation of classical methods in analyzing CRTs and provide a fresh perspective on treatment effects with a new inferential target. More broadly, we expand the conformal inference toolkit to accommodate clustered data and their covariate subgroups, addressing model-robust finite-sample validity under a broader set of data-generating distributions.

Although our data example in Section 6 includes a large number of clusters, our proposed methods are not confined to a large number of clusters, given appropriate adjustments of the target coverage probability. As discussed in Sections 3, for achieving 90% coverage probability of the conformal interval for the cluster-level treatment effects, we need at least 10 clusters per arm for numerically stable calibration, and our simulation shows that the conformal interval is valid but moderately conservative given  $m = 30$  and  $\pi = 0.5$ . Given



fewer clusters, e.g.,  $m = 20$ , targeting 90% coverage probability will only result in intervals spanning the entire real line, and informative intervals are possible with a lower target coverage probability (say 80%). In practice, we recommend setting  $\alpha = 0.05$  if  $m \geq 80$ ,  $\alpha = 0.1$  if  $40 \leq m < 80$ , and  $\alpha = 0.2$  if  $20 \leq m < 40$  given  $\pi = 0.5$ . If  $10 < m < 20$ , we can still construct the 80% conformal interval for the individual-level treatment effect, while it may be challenging to make conformal causal inference given  $m \leq 10$ . Conformal causal inference with an extremely small number of clusters is a topic of future research.

## References

- Alaa, A., Ahmad, Z., and van der Laan, M. (2023). Conformal meta-learners for predictive inference of individual treatment effects. *arXiv preprint arXiv:2308.14895*.
- Balzer, L. B., Petersen, M. L., van der Laan, M. J., and Collaboration, S. (2016). Targeted estimation and inference for the sample average treatment effect in trials with and without pair-matching. *Statistics in Medicine*, 35(21):3717–3732.
- Balzer, L. B., van der Laan, M., Ayieko, J., Kanya, M., Chamie, G., Schwab, J., Havlir, D. V., and Petersen, M. L. (2023). Two-stage TMLE to reduce bias and improve efficiency in cluster randomized trials. *Biostatistics*, 24(2):502–517.
- Barber, R. F., Candès, E. J., Ramdas, A., and Tibshirani, R. J. (2021). Predictive inference with the jackknife+. *The Annals of Statistics*, 49(1):486 – 507.
- Benitez, A., Petersen, M. L., van der Laan, M. J., Santos, N., Butrick, E., Walker, D., Ghosh, R., Otieno, P., Waiswa, P., and Balzer, L. B. (2023). Defining and estimating effects in cluster randomized trials: A methods comparison. *Statistics in Medicine*, 42(19):3443–3466.
- Breiman, L. (2001). Random forests. *Machine learning*, 45:5–32.

- Campbell, M. K., Fayers, P. M., and Grimshaw, J. M. (2005). Determinants of the intraclass correlation coefficient in cluster randomized trials: the case of implementation research. *Clinical Trials*, 2(2):99–107.
- Crespi, C. M., Wong, W. K., and Mishra, S. I. (2009). Using second-order generalized estimating equations to model heterogeneous intraclass correlation in cluster-randomized trials. *Statistics in Medicine*, 28(5):814–827.
- DeBar, L., Mayhew, M., Benes, L., Bonifay, A., Deyo, R. A., Elder, C. R., Keefe, F. J., Leo, M. C., McMullen, C., Owen-Smith, A., et al. (2022). A primary care-based cognitive behavioral therapy intervention for long-term opioid users with chronic pain: a randomized pragmatic trial. *Annals of Internal Medicine*, 175(1):46–55.
- Ding, P. and Keele, L. (2018). Rank tests in unmatched clustered randomized trials applied to a study of teacher training. *The Annals of Applied Statistics*, 12(4):2151–2174.
- Hore, R. and Barber, R. F. (2023). Conformal prediction with local weights: randomization enables local guarantees. *arXiv preprint arXiv:2310.07850*.
- Ivers, N., Taljaard, M., Dixon, S., Bennett, C., McRae, A., Taleban, J., Skea, Z., Brehaut, J., Boruch, R., Eccles, M., et al. (2011). Impact of consort extension for cluster randomised trials on quality of reporting and study methodology: review of random sample of 300 trials, 2000-8. *Bmj*, 343.
- Jin, Y., Ren, Z., and Candès, E. J. (2023). Sensitivity analysis of individual treatment effects: A robust conformal inference approach. *Proceedings of the National Academy of Sciences*, 120(6):e2214889120.
- Kahan, B. C., Li, F., Copas, A. J., and Harhay, M. O. (2023). Estimands in cluster-randomized trials: choosing analyses that answer the right question. *International Journal of Epidemiology*, 52(1):107–118.

- Lee, Y., Barber, R. F., and Willett, R. (2023). Distribution-free inference with hierarchical data. *arXiv preprint arXiv:2306.06342*.
- Lei, J., G’Sell, M., Rinaldo, A., Tibshirani, R. J., and Wasserman, L. (2018). Distribution-free predictive inference for regression. *Journal of the American Statistical Association*, 113(523):1094–1111.
- Lei, J. and Wasserman, L. (2014). Distribution-free prediction bands for non-parametric regression. *Journal of the Royal Statistical Society Series B: Statistical Methodology*, 76(1):71–96.
- Lei, L. and Candès, E. J. (2021). Conformal inference of counterfactuals and individual treatment effects. *Journal of the Royal Statistical Society Series B: Statistical Methodology*, 83(5):911–938.
- Murray, D. M. et al. (1998). *Design and Analysis of Group-Randomized Trials*, volume 29. Oxford University Press, USA.
- Papadopoulos, H., Proedrou, K., Vovk, V., and Gammerman, A. (2002). Inductive confidence machines for regression. In *Machine Learning: ECML 2002: 13th European Conference on Machine Learning Helsinki, Finland, August 19–23, 2002 Proceedings 13*, pages 345–356. Springer.
- Qiu, H., Dobriban, E., and Tchetgen, E. T. (2022). Prediction sets adaptive to unknown covariate shift. *arXiv preprint arXiv:2203.06126*.
- Rabideau, D. J. and Wang, R. (2021). Randomization-based confidence intervals for cluster randomized trials. *Biostatistics*, 22(4):913–927.
- Small, D. S., Ten Have, T. R., and Rosenbaum, P. R. (2008). Randomization inference in a group-randomized trial of treatments for depression: covariate adjustment, noncompliance, and quantile effects. *Journal of the American Statistical Association*, 103(481):271–279.

- Su, F. and Ding, P. (2021). Model-assisted analyses of cluster-randomized experiments. *Journal of the Royal Statistical Society, Series B*, 83(5):994–1015.
- Tibshirani, R. J., Foygel Barber, R., Candès, E., and Ramdas, A. (2019). Conformal prediction under covariate shift. *Advances in neural information processing systems*, 32:1–11.
- van der Laan, M. J., Polley, E. C., and Hubbard, A. E. (2007). Super learner. *Statistical Applications in Genetics and Molecular Biology*, 6(1):1–21.
- Vovk, V., Gammerman, A., and Shafer, G. (2005). *Algorithmic learning in a random world*, volume 29. Springer.
- Wang, B., Harhay, M. O., Small, D. S., Morris, T. P., and Li, F. (2021). On the mixed-model analysis of covariance in cluster-randomized trials. *arXiv preprint arXiv:2112.00832*.
- Wang, B., Park, C., Small, D. S., and Li, F. (2023). Model-robust and efficient inference for cluster-randomized experiments. *Journal of the American Statistical Association*.
- Yang, Y., Kuchibhotla, A. K., and Tchetgen, E. T. (2022). Doubly robust calibration of prediction sets under covariate shift. *arXiv preprint arXiv:2203.01761*.
- Yin, M., Shi, C., Wang, Y., and Blei, D. M. (2022). Conformal sensitivity analysis for individual treatment effects. *Journal of the American Statistical Association*, pages 1–14.
- Zhang, K., Traskin, M., and Small, D. S. (2012). A powerful and robust test statistic for randomization inference in group-randomized trials with matched pairs of groups. *Biometrics*, 68(1):75–84.

# Supporting Information for “Conformal causal inference for cluster randomized trials: model-robust inference without asymptotic approximations”

In Section [A](#), we provide the proofs for our theoretical results. In Section [B](#), we provide the nested approach for constructing conformal intervals based on CRTs. In Section [C](#), we provide additional simulation results. The R code for reproducing all simulation and data analysis is available at <https://github.com/BingkaiWang/CRT-conformal>.

## A Proofs

### A.1 Proof of Theorem 1

*Proof of Theorem 1.* Since  $\tilde{C}_C(\bar{O}_{\text{test}}) = (-1)^{A_{\text{test}}+1}\{\bar{Y}_{\text{test}} - \tilde{C}_{C,1-A_{\text{test}}}(\bar{B}_{\text{test}})\}$  and  $\bar{Y}_{\text{test}} = A_{\text{test}}\bar{Y}_{\text{test}}(1) + (1 - A_{\text{test}})\bar{Y}_{\text{test}}(0)$ , we have

$$\begin{aligned} & P\left\{\bar{Y}_{\text{test}}(1) - \bar{Y}_{\text{test}}(0) \notin \tilde{C}_C(\bar{O}_{\text{test}}) \mid \bar{B}_{\text{test}} \in \Omega_C\right\} \\ &= \sum_{a=0}^1 P\left\{\bar{Y}_{\text{test}}(1) - \bar{Y}_{\text{test}}(0) \notin \tilde{C}_C(\bar{O}_{\text{test}}), A_{\text{test}} = a \mid \bar{B}_{\text{test}} \in \Omega_C\right\} \\ &= \sum_{a=0}^1 P\left\{\bar{Y}_{\text{test}}(a) \notin \tilde{C}_{C,a}(\bar{B}_{\text{test}}), A_{\text{test}} = 1 - a \mid \bar{B}_{\text{test}} \in \Omega_C\right\} \\ &\leq \sum_{a=0}^1 P\left\{\bar{Y}_{\text{test}}(a) \notin \tilde{C}_{C,a}(\bar{B}_{\text{test}}) \mid \bar{B}_{\text{test}} \in \Omega_C\right\}. \end{aligned}$$

Therefore, it remains to show  $P\left\{\bar{Y}_{\text{test}}(a) \notin \tilde{C}_{C,a}(\bar{B}_{\text{test}}) \mid \bar{B}_{\text{test}} \in \Omega_C\right\} \leq \alpha$  for  $a = 0, 1$ .

Denote  $\mathcal{I} = \mathcal{I}_{ca}(a) \cup \{\text{test}\}$ . By Assumptions 1-2 and the additional assumption in Theorem 1,  $\{(\bar{Y}_i(a), \bar{B}_i) : i \in \mathcal{I}\}$  are i.i.d. given  $\bar{B}_i \in \Omega_C$ . Of note, here we use Assumption 2 to obtain  $(\bar{Y}_i(a), \bar{B}_i) | (A_i = a, \bar{B}_i \in \Omega_C)$  is identically distributed as  $(\bar{Y}_i(a), \bar{B}_i) | (\bar{B}_i \in \Omega_C)$  for  $i \in \mathcal{I}_{ca}(a)$ . Since  $\hat{f}_a$  is a function of the training data, which are independent of the calibration data and test data, then  $\{s(\bar{B}_i, \bar{Y}_i(a)), i \in \mathcal{I}\}$  are also i.i.d. conditioning on the training fold and  $\bar{B}_i \in \Omega_C$ . Then,

$$P \left\{ s(\bar{B}_{\text{test}}, \bar{Y}_{\text{test}}(a)) \leq \text{Quantile}_{1-\alpha} \left( \frac{1}{|\mathcal{I}|} \sum_{i \in \mathcal{I}} \delta_{s(\bar{B}_i, \bar{Y}_i(a))} \right) \middle| \bar{B}_{\text{test}} \in \Omega_C \right\} \geq 1 - \alpha.$$

Since the quantile of an empirical distribution does not decrease if we replace one sample by  $+\infty$ , we also have

$$P \left\{ s(\bar{B}_{\text{test}}, \bar{Y}_{\text{test}}(a)) \leq \text{Quantile}_{1-\alpha} \left( \frac{1}{|\mathcal{I}_{ca}(a)| + 1} \sum_{i \in \mathcal{I}_{ca}(a)} \delta_{s(\bar{B}_i, \bar{Y}_i(a))} + \delta_{+\infty} \right) \middle| \bar{B}_{\text{test}} \in \Omega_C \right\} \geq 1 - \alpha.$$

Since  $\bar{Y}_i(a) = \bar{Y}_i$  for  $i \in \mathcal{I}_{ca}(a)$ , we have

$$\text{Quantile}_{1-\alpha} \left( \frac{1}{|\mathcal{I}_{ca}(a)| + 1} \sum_{i \in \mathcal{I}_{ca}(a)} \delta_{s(\bar{B}_i, \bar{Y}_i(a))} + \delta_{+\infty} \right) = \text{Quantile}_{1-\alpha}(\hat{F}) = \hat{q}_{1-\alpha}(a).$$

Therefore,

$$P \left( \bar{Y}_{\text{test}}(a) \in \tilde{C}_{C,a}(\bar{B}_{\text{test}}) \middle| \bar{B}_{\text{test}} \in \Omega_C \right) = P \left( s(\bar{B}_{\text{test}}, \bar{Y}_{\text{test}}(a)) \leq \hat{q}_{1-\alpha}(a) \middle| \bar{B}_{\text{test}} \in \Omega_C \right) \geq 1 - \alpha,$$

which completes the proof.  $\square$

## A.2 Proof of Theorem 2

**Lemma 1.** Denote  $M_i = \sum_{j=1}^{N_i} I\{B_{ij} \in \Omega_I\}$  and  $1 \leq j_1 \leq \dots \leq j_{M_i} \leq N_i$  be the ordered indices such that  $B_{ij_k} \in \Omega_I$  for  $k = 1, \dots, M_i$ . Letting  $e_{ij_k}$  be a length- $N_i$  vector with the  $j_k$ -th entry 1 and the rest zero, we define a matrix  $D_i = [e_{ij_1}, \dots, e_{ij_{M_i}}] \in \mathbb{R}^{N_i \times M_i}$  and

$\widetilde{W}_i = D_i^\top W_i$ , where  $W_i = (V_{i1}^\top, \dots, V_{iN_i}^\top)^\top \in \mathbb{R}^{N_i \times (p+2)}$  for  $V_{ij} = (Y_{ij}(1), Y_{ij}(0), B_{ij}) \in \mathbb{R}^{p+2}$ . In other words,  $\widetilde{W}_i$  is the data from cluster  $i$  after filtering out individuals with  $B_{ij} \notin \Omega_I$ . For notational convenience, we denote the  $j$ -th row of  $\widetilde{W}_i$  as  $\widetilde{V}_{ij}$ . Under Assumptions 1 and 3, we have

(a)  $(\widetilde{W}_1, \dots, \widetilde{W}_m)$  are independent and identically distributed.

(b) Within  $\widetilde{W}_i$ , the distribution of  $(\widetilde{V}_{i1}, \dots, \widetilde{V}_{iM_i})$  is exchangeable conditioning on  $M_i$ .

(c) Given the above results,  $\widetilde{V}_{ij}$  has the same distribution as  $V_{ij} | (B_{ij} \in \Omega_I)$  for any  $j$ . It implies that  $E[f(\widetilde{V}_{ij}, U)] = E[f(V_{ij}, U) | B_{ij} \in \Omega_I]$  for any  $U$  that is independent of  $(V_{ij}, \widetilde{V}_{ij})$  and any integrable function  $f$ .

*Proof of Lemma 1.* To prove (a), we observe that  $D_i$  is a deterministic function of  $W_i$  and  $\Omega_I$ . Since  $\widetilde{W}_i = D_i^\top W_i$ , Assumption 1 implies that  $(\widetilde{W}_1, \dots, \widetilde{W}_m)$  are independent and identically distributed.

To prove (b), conditional on  $N_i$ , we define  $Q_i = (I\{B_{i1} \in \Omega_I\}, \dots, I\{B_{iN_i} \in \Omega_I\})$ . We first prove that  $(\widetilde{V}_{i1}, \dots, \widetilde{V}_{iM_i}) | Q_i = q, M_i = m$  are exchangeable.

Without loss of generality, we assume  $B_{ij}, j = 1, \dots, m \in \Omega_I$  (the first  $m$  elements). For any measurable sets  $A_1, \dots, A_m$ , the conditional distribution of  $(\widetilde{V}_{i1}, \dots, \widetilde{V}_{iM_i}) | Q_i = q, M_i = m$  is given by

$$(i) := P(V_{i1} \in A_1, \dots, V_{im} \in A_m | V_{i1} \in B, \dots, V_{im} \in B, V_{i(m+1)} \in C, \dots, V_{iN_i} \in C).$$

Here we denote the domain of  $(Y(1), Y(0))$  as  $\mathcal{D}_Y \in \mathbb{R}^2$  and let  $B = \mathcal{D}_Y \times \Omega_I$  and  $C = \mathcal{D}_Y \times \Omega_I^c$ . It holds that

$$(i) = \frac{P(V_{i1} \in A_1 \cap B, \dots, V_{im} \in A_m \cap B, V_{i(m+1)} \in C, \dots, V_{iN_i} \in C)}{P(V_{i1} \in B, \dots, V_{im} \in B, V_{i(m+1)} \in C, \dots, V_{iN_i} \in C)}$$

Since conditional on  $N_i$ ,  $(V_{i1}, \dots, V_{iN_i})$  are exchangeable, for any  $\sigma \in S_m$ , we obtain

$$\begin{aligned}
(i) &= \frac{P(V_{i\sigma(1)} \in A_1 \cap B, \dots, V_{i\sigma(m)} \in A_m \cap B, V_{i(m+1)} \in C, \dots, V_{iN_i} \in C)}{P(V_{i1} \in B, \dots, V_{im} \in B, V_{i(m+1)} \in C)} \\
&= \frac{P(V_{i\sigma(1)} \in A_1, \dots, V_{i\sigma(m)} \in A_m, V_{i1} \in B, \dots, V_{im} \in B, V_{i(m+1)} \in C, \dots, V_{iN_i} \in C)}{P(V_{i1} \in B, \dots, V_{im} \in B, V_{i(m+1)} \in C)} \\
&= P(V_{i\sigma(1)} \in A_1, \dots, V_{i\sigma(m)} \in A_m | V_{i1} \in B, \dots, V_{im} \in B, V_{i(m+1)} \in C, \dots, V_{iN_i} \in C).
\end{aligned}$$

Therefore, we have  $[(\tilde{V}_{i1}, \dots, \tilde{V}_{iM_i}) | Q_i = q, M_i = m] \stackrel{d}{=} [(\tilde{V}_{i\sigma(1)}, \dots, \tilde{V}_{i\sigma(M_i)}) | Q_i = q, M_i = m]$  for any  $\sigma \in S_m$ .

We next prove the exchangeability by only conditioning on  $M_i = m$ .

We know that for any  $\sigma \in S_m$

$$\begin{aligned}
&P(\tilde{V}_{i\sigma(1)}, \dots, \tilde{V}_{i\sigma(M_i)} \in A_1 \times \dots \times A_m | M_i = m) \\
&= \sum_{Q_i=q} P(\tilde{V}_{i\sigma(1)}, \dots, \tilde{V}_{i\sigma(M_i)} \in A_1 \times \dots \times A_m | Q_i = q, M_i = m) \cdot P(Q_i = q | M_i = m) \\
&= \sum_{Q_i=q} P(\tilde{V}_{i1}, \dots, \tilde{V}_{iM_i} \in A_1 \times \dots \times A_m | Q_i = q, M_i = m) \cdot P(Q_i = q | M_i = m) \\
&= P(\tilde{V}_{i1}, \dots, \tilde{V}_{iM_i} \in A_1 \times \dots \times A_m | M_i = m).
\end{aligned}$$

We then conclude our proof of (b).

Finally, we prove (c). By definition,  $\tilde{V}_{ij}$  is equal to  $V_{ij'}$  for some  $j'$  such that  $B_{ij'} \in \Omega_I$ . Therefore,  $\tilde{V}_{ij} \stackrel{d}{=} V_{ij'} | (B_{ij'} \in \Omega_I)$ . By the exchangeability of  $W_i$ , we have  $\tilde{V}_{ij} \stackrel{d}{=} V_{ij} | (B_{ij} \in \Omega_I)$ .



In addition,

$$\begin{aligned}
E[f(V_{ij}, U)|B_{ij} \in \Omega_I] &= \int f(V_{ij}, U)dP(V_{ij}, U|B_{ij} \in \Omega_I) \\
&= \int f(V_{ij}, U)d\{P(V_{ij}|B_{ij} \in \Omega_I)P(U)\} \\
&= \int f(\tilde{V}_{ij}, U)d\{P(\tilde{V}_{ij})P(U)\} \\
&= \int f(\tilde{V}_{ij}, U)dP(\tilde{V}_{ij}, U) \\
&= E[f(\tilde{V}_{ij}, U)],
\end{aligned}$$

where the second and fourth equation uses the independence between  $U$  and  $(V_{ij}, \tilde{V}_{ij})$ , and the third equation results from  $\tilde{V}_{ij} \stackrel{d}{=} V_{ij}|(B_{ij} \in \Omega_I)$ .  $\square$

*Proof of Theorem 2.* Since  $\tilde{C}_I(O_{\text{test}}) = (-1)^{A_{\text{test}}+1}\{Y_{\text{test}} - \tilde{C}_{I,1-A_{\text{test}}}(B_{\text{test}})\}$  and  $Y_{\text{test}} = A_{\text{test}}Y_{\text{test}}(1) + (1 - A_{\text{test}})Y_{\text{test}}(0)$ , we have

$$\begin{aligned}
&P\left\{Y_{\text{test}}(1) - Y_{\text{test}}(0) \notin \tilde{C}_I(O_{\text{test}}) \middle| B_{\text{test}} \in \Omega_C\right\} \\
&= \sum_{a=0}^1 P\left\{Y_{\text{test}}(1) - Y_{\text{test}}(0) \notin \tilde{C}_I(O_{\text{test}}), A_{\text{test}} = a \middle| B_{\text{test}} \in \Omega_C\right\} \\
&= \sum_{a=0}^1 P\left\{Y_{\text{test}}(a) \notin \tilde{C}_{I,a}(B_{\text{test}}), A_{\text{test}} = 1 - a \middle| B_{\text{test}} \in \Omega_C\right\} \\
&\leq \sum_{a=0}^1 P\left\{Y_{\text{test}}(a) \notin \tilde{C}_{I,a}(B_{\text{test}}) \middle| B_{\text{test}} \in \Omega_C\right\}.
\end{aligned}$$

Therefore, it remains to show  $P\left\{Y_{\text{test}}(a) \notin \tilde{C}_{I,a}(B_{\text{test}}) \middle| B_{\text{test}} \in \Omega_C\right\} \leq \alpha$  for  $a = 0, 1$ .

To this end, we denote  $W_{m+1}$  as a new cluster independently sampled from  $\mathcal{P}^W$ . By construction,  $(Y_{\text{test}}(1), Y_{\text{test}}(0), B_{\text{test}})$  comes from an arbitrary individual in this cluster. By Assumption 3,  $(Y_{\text{test}}(1), Y_{\text{test}}(0), B_{\text{test}})$  is identically distributed as  $V_{m+1,1} = (Y_{m+1,1}(1), Y_{m+1,1}(0), B_{m+1,1})$ , where  $V_{m+1,j}$  is the  $j$ -th row of  $W_{m+1}$ . Therefore, our goal is to show  $P\left\{Y_{m+1,1}(a) \notin \tilde{C}_{I,a}(B_{m+1,1}) \middle| B_{m+1,1} \in \Omega_C\right\} \leq \alpha$ .

$\tilde{C}_{I,a}(B_{m+1,1}) \Big| B_{m+1,1} \in \Omega_C \Big\} \leq \alpha$  for  $a = 0, 1$ . To further simplify the goal, we denote  $\tilde{W}_{m+1}$  as the new cluster after we filter out individuals with  $B_{m+1,j} \notin \Omega_I$  and let  $\tilde{V}_{m+1,j} = (\tilde{Y}_{m+1,j}(1), \tilde{Y}_{m+1,j}(0), \tilde{B}_{m+1,j})$  denote the  $j$ -th row of  $\tilde{W}_{m+1}$ . (See Lemma 1 for the detailed construction for  $\tilde{W}_{m+1}$ ). By Lemma 1 (c),  $\tilde{V}_{m+1,1}$  is identically distributed as  $V_{m+1,1} | (B_{m+1,1} \in \Omega_I)$ . Since  $\tilde{C}_{I,a}$  is a function of  $\{W_i : i = 1, \dots, m, A_i = a\}$ , which are independent of  $W_{m+1}$ , Lemma 1(c) further implies

$$P \left\{ Y_{m+1,1}(a) \notin \tilde{C}_{I,a}(B_{m+1,1}) \Big| B_{m+1,1} \in \Omega_C \right\} = P \left\{ \tilde{Y}_{m+1,1}(a) \notin \tilde{C}_{I,a}(\tilde{B}_{m+1,1}) \right\}.$$

This result yields our final goal to show  $P \left\{ \tilde{Y}_{m+1,1}(a) \notin \tilde{C}_{I,a}(\tilde{B}_{m+1,1}) \right\} \leq \alpha$ .

Next, we denote the calibration data  $\mathcal{O}_{ca}(a) = \{\tilde{W}_i : i \in \mathcal{I}_{ca}(a)\}$ . Like  $\tilde{W}_{m+1}$ ,  $\tilde{W}_i$  contains those individuals in  $W_i$  with  $B_{ij} \in \Omega_I$ . By Assumptions 1-2 and Lemma 1(a),  $\{\tilde{W}_i : i \in \mathcal{I}\}$  are i.i.d., where  $\mathcal{I} = \mathcal{I}_{ca}(a) \cup \{m+1\}$ . Within each  $\tilde{W}_i$ , Lemma 1 (b) implies that  $(\tilde{V}_{i1}, \dots, \tilde{V}_{iM_i})$  are exchangeable conditioning on  $M_i$  within each cluster.

We define a function

$$q_{1-\alpha}(\{\tilde{W}_i, i \in \mathcal{I}\}) = \text{Quantile}_{1-\alpha} \left( \frac{1}{|\mathcal{I}|} \sum_{i \in \mathcal{I}} \frac{1}{M_i} \sum_{j=1}^{M_i} \delta_{s(\tilde{B}_{ij}, \tilde{Y}_{ij}(a))} \right),$$

which is the  $(1 - \alpha)$ -quantile of the weighted empirical distribution for the calibration data and new cluster. By definition of the quantile function, we have, for any  $i \in \mathcal{I}$  and  $j \in \{1, \dots, M_i\}$ ,

$$\frac{1}{|\mathcal{I}|} \sum_{i \in \mathcal{I}} \frac{1}{M_i} \sum_{j=1}^{M_i} I \left\{ s(\tilde{B}_{ij}, \tilde{Y}_{ij}(a)) \leq q_{1-\alpha}(\{\tilde{W}_i, i \in \mathcal{I}\}) \right\} \geq 1 - \alpha.$$

Consider any permutation  $\sigma$  map on  $(1, \dots, M_{m+1})$ . Since we have shown that each  $\tilde{W}_i$  is exchangeable given  $M_i$ , we have, for each  $i \in \mathcal{I}$ ,

$$I \left\{ s(\tilde{B}_{ij}, \tilde{Y}_{ij}(a)) \leq q_{1-\alpha}(\{\tilde{W}_i, i \in \mathcal{I}\}) \right\} \stackrel{d}{=} I \left\{ s(\tilde{B}_{i\sigma(j)}, \tilde{Y}_{i\sigma(j)}(a)) \leq q_{1-\alpha}(\{\tilde{W}_{i'}, i' \in \mathcal{I}, i' \neq i\} \cup \{\sigma(\tilde{W}_i)\}) \right\},$$

conditioning on the training fold and  $M_i$ . Since the weighted empirical distribution is invariant to within-cluster permutations, we have  $q_{1-\alpha}(\{\widetilde{W}_{i'}, i' \in \mathcal{I}, i' \neq i\} \cup \{\sigma(\widetilde{W}_i)\}) = q_{1-\alpha}(\{\widetilde{W}_i, \in \mathcal{I}\})$ . Combined with the fact that the training fold is independent of the calibration data and the test data, we have

$$E \left[ I \left\{ s(\widetilde{B}_{ij}, \widetilde{Y}_{ij}(a)) \leq q_{1-\alpha}(\{\widetilde{W}_i, \in \mathcal{I}\}) \right\} \middle| M_i \right] = E \left[ I \left\{ s(\widetilde{B}_{i1}, \widetilde{Y}_{i1}(a)) \leq q_{1-\alpha}(\{\widetilde{W}_i, \in \mathcal{I}\}) \right\} \middle| M_i \right]$$

by choosing permutations  $\sigma$  with  $\sigma(j) = 1$ . After averaging over  $i$  and marginalizing over  $M_i$ , we have

$$E \left[ I \left\{ s(\widetilde{B}_{i1}, \widetilde{Y}_{i1}(a)) \leq q_{1-\alpha}(\{\widetilde{W}_i, \in \mathcal{I}\}) \right\} \right] = E \left[ \frac{1}{M_i} \sum_{j=1}^{M_i} I \left\{ s(\widetilde{B}_{ij}, \widetilde{Y}_{ij}(a)) \leq q_{1-\alpha}(\{\widetilde{W}_i, \in \mathcal{I}\}) \right\} \right].$$

Since we have shown that  $\widetilde{W}_i$  are i.i.d., we also have

$$\begin{aligned} & E \left[ \frac{1}{M_i} \sum_{j=1}^{M_i} I \left\{ s(\widetilde{B}_{ij}, \widetilde{Y}_{ij}(a)) \leq q_{1-\alpha}(\{\widetilde{W}_i, \in \mathcal{I}\}) \right\} \right] \\ &= E \left[ \frac{1}{|\mathcal{I}|} \sum_{i \in \mathcal{I}} \frac{1}{M_i} \sum_{j=1}^{M_i} I \left\{ s(\widetilde{B}_{ij}, \widetilde{Y}_{ij}(a)) \leq q_{1-\alpha}(\{\widetilde{W}_i, \in \mathcal{I}\}) \right\} \right]. \end{aligned}$$

Taken together, we get

$$\begin{aligned} & E \left[ I \left\{ s(\widetilde{B}_{m+1,1}, \widetilde{Y}_{m+1,1}(a)) \leq q_{1-\alpha}(\{\widetilde{W}_i, \in \mathcal{I}\}) \right\} \right] \\ &= E \left[ \frac{1}{|\mathcal{I}|} \sum_{i \in \mathcal{I}} \frac{1}{M_i} \sum_{j=1}^{M_i} I \left\{ s(\widetilde{B}_{ij}, \widetilde{Y}_{ij}(a)) \leq q_{1-\alpha}(\{\widetilde{W}_i, \in \mathcal{I}\}) \right\} \right] \\ &\geq 1 - \alpha. \end{aligned}$$

Finally, we need to connect  $q_{1-\alpha}(\{\widetilde{W}_i, \in \mathcal{I}\})$  to  $\widehat{q}_{1-\alpha}$  defined in Algorithm 3. Since replacing some point masses in the weighted empirical distribution by  $\delta_{+\infty}$  does not decrease the  $(1 - \alpha)$ -quantile, we have  $q_{1-\alpha}(\{\widetilde{W}_i, \in \mathcal{I}\}) \leq \widehat{q}_{1-\alpha}$ , which implies  $P(s(\widetilde{B}_{m+1,1}, \widetilde{Y}_{m+1,1}(a)) \leq \widehat{q}_{1-\alpha}) \geq 1 - \alpha$ . Since we defined  $\widetilde{C}_{I,a}(B) = \{y \in \mathbb{R} : |y - \widehat{f}_a(B)| \leq \widehat{q}_{1-\alpha}(a)\}$ , then

the event  $Y_{m+1,1} \in \tilde{C}_{I,a}(B_{m+1,1})$  is equal to  $s(\tilde{B}_{m+1,1}, \tilde{Y}_{m+1,1}(a)) \leq \hat{q}_{1-\alpha}$ , which implies  $P \left\{ \tilde{Y}_{m+1,1}(a) \notin \tilde{C}_{I,a}(\tilde{B}_{m+1,1}) \right\} \leq \alpha$ . This completes the proof.  $\square$

## B Nested approaches to construct conformal intervals

### B.1 Cluster-level treatment effect

---

**Algorithm B.1** Computing the conformal interval  $\tilde{C}_C(\bar{B})$  for cluster-level treatment effects.

**Input:** Cluster-level data  $\{(\bar{Y}_i, A_i, \bar{B}_i) : i = 1, \dots, m\}$ , a test point  $\bar{B}_{\text{test}}$ , a prediction model  $f_a(\bar{B})$  for  $\bar{Y}(a)$ ,  $a \in \{0, 1\}$ , prediction models  $\{m^L(\bar{B}), m^R(\bar{B})\}$  for the  $(\alpha/2, 1 - \alpha/2)$ -quantiles of  $\bar{Y}(1) - \bar{Y}(0)$ , a covariate-subgroup of interest  $\Omega_C$ , and levels  $(\alpha, \gamma)$ .

**Procedure:**

1. For  $a = 0, 1$ , randomly split the arm- $a$  covariate-subgroup data  $\{(\bar{Y}_i, \bar{B}_i) : i = 1, \dots, m, A_i = a, \bar{B}_i \in \Omega_C\}$  into a training fold  $\mathcal{O}_{tr}(a)$ , and a calibration fold  $\mathcal{O}_{ca}(a)$  with index set  $\mathcal{I}_{ca}(a)$ .

2. Use the training fold to run Step 1 of Algorithm 1 of the main paper and obtain the  $(1 - \alpha)$  conformal interval  $\tilde{C}_{C,a}(\bar{B})$  for  $\bar{Y}(a)$ ,  $a = 0, 1$ .

3. For each  $i = 1, \dots, m$ , define  $\bar{C}_i = A_i\{\bar{Y}_i - \tilde{C}_{C,0}(\bar{B}_i)\} + (1 - A_i)\{\tilde{C}_{C,1}(\bar{B}_i) - \bar{Y}_i\}$  and denote  $\bar{C}_i = [\bar{C}_i^L, \bar{C}_i^R]$ .

4. Train prediction models  $m^L(\bar{B})$  for  $\bar{C}^L$  and  $m^R(\bar{B})$  for  $\bar{C}^R$  using all data in the training fold  $\{\mathcal{O}_{tr}(a) : a = 0, 1\}$ , and obtain the estimated models  $\hat{m}^L(\bar{B})$  and  $\hat{m}^R(\bar{B})$ .

5. For each  $i \in \mathcal{I}_{ca}(1) \cup \mathcal{I}_{ca}(0)$ , compute the non-conformity score

$$s^*(\bar{B}_i, \bar{C}_i) = \max\{\hat{m}^L(\bar{B}_i) - \bar{C}_i^L, \bar{C}_i^R - \hat{m}^R(\bar{B}_i)\}.$$

6. Compute the  $1 - \gamma$  quantile  $\hat{q}_{1-\gamma}^*$  of the distribution

$$\hat{F}^* = \frac{1}{|\mathcal{I}_{ca}(1)| + |\mathcal{I}_{ca}(0)| + 1} \left\{ \sum_{i \in \mathcal{I}_{ca}(1) \cup \mathcal{I}_{ca}(0)} \delta_{s^*(\bar{B}_i, \bar{C}_i)} + \delta_{+\infty} \right\}.$$

**Output:**  $\tilde{C}_C(\bar{B}_{\text{test}}) = [\hat{m}^L(\bar{B}_{\text{test}}) - \hat{q}_{1-\gamma}^*, \hat{m}^R(\bar{B}_{\text{test}}) + \hat{q}_{1-\gamma}^*]$ .

---

**Theorem B.1.** Assume Assumptions 1-2 and that  $(\bar{Y}_{\text{test}}(1), \bar{Y}_{\text{test}}(0), \bar{B}_{\text{test}})$  is an independent from the distribution induced by  $\mathcal{P}^W$ . Then, the  $\tilde{\mathcal{C}}_C(\bar{B}_{\text{test}})$  output by Algorithm B.1 satisfies

$$P\left\{\bar{Y}_{\text{test}}(1) - \bar{Y}_{\text{test}}(0) \in \tilde{\mathcal{C}}_C(\bar{B}_{\text{test}}) \middle| \bar{B}_{\text{test}} \in \Omega_C\right\} \geq 1 - \alpha - \gamma \quad (1)$$

for any set  $\Omega_C$  in the support of  $\bar{B}_{\text{test}}$  with a positive measure.

*Proof of Theorem B.1.* Following the proof of Theorem 1, we have  $P\left\{\bar{Y}(a) \notin \tilde{\mathcal{C}}_{C,a}(\bar{B}) \middle| \bar{B} \in \Omega_C\right\} \leq \alpha$  for  $a = 0, 1$ . Since Assumption 2 implies that  $A$  is independent of  $(\bar{Y}(a), \bar{B})$ , then

$$\begin{aligned} & P\left\{\bar{Y}(1) - \bar{Y}(0) \in A\{\bar{Y} - \tilde{\mathcal{C}}_{C,0}(\bar{B})\} + (1 - A)\{\tilde{\mathcal{C}}_{C,1}(\bar{B}) - \bar{Y}\} \middle| \bar{B} \in \Omega_C\right\} \\ &= \sum_{a=0}^1 P\left\{\bar{Y}(a) \in \tilde{\mathcal{C}}_{C,a}(\bar{B}), A = a \middle| \bar{B} \in \Omega_C\right\} \\ &= \sum_{a=0}^1 P\left\{\bar{Y}(a) \in \tilde{\mathcal{C}}_{C,a}(\bar{B}) \middle| \bar{B} \in \Omega_C\right\} P(A = a) \\ &\geq 1 - \alpha. \end{aligned}$$

Therefore, by defining  $\bar{C}_i = A_i\{\bar{Y}_i - \tilde{\mathcal{C}}_{C,0}(\bar{B}_i)\} + (1 - A_i)\{\tilde{\mathcal{C}}_{C,1}(\bar{B}_i) - \bar{Y}_i\}$ , we have  $\bar{C}_i = [\bar{C}_i^L, \bar{C}_i^R]$  representing the  $(\alpha/2, 1 - \alpha/2)$ -quantile of  $\bar{Y}_i(1) - \bar{Y}_i(0)$ .

Next, we independently generate  $A_{\text{test}}$  from  $\mathcal{P}^A$  and compute  $\bar{C}_{\text{test}} = A_{\text{test}}\{\bar{Y}_{\text{test}} - \tilde{\mathcal{C}}_{C,0}(\bar{B}_{\text{test}})\} + (1 - A_{\text{test}})\{\tilde{\mathcal{C}}_{C,1}(\bar{B}_{\text{test}}) - \bar{Y}_{\text{test}}\}$ . As a result,  $(\bar{B}_{\text{test}}, \bar{C}_{\text{test}})$  is independent and identically distributed as  $(\bar{B}_i, \bar{C}_i)$ . We observe that  $\tilde{\mathcal{C}}_{C,a}, \hat{m}^L, \hat{m}^R$  are all functions of the training folds  $\{\mathcal{O}_{tr}(a) : a = 0, 1\}$ , which are independent of the calibration data and test data. Denoting  $\mathcal{I} = \mathcal{I}_{ca}(1) \cup \mathcal{I}_{ca}(0) \cup \{\text{test}\}$ , by Assumptions 1-2,  $\{s^*(\bar{B}_i, \bar{C}_i), i \in \mathcal{I}\}$  are i.i.d. conditioning on the training folds and  $\bar{B}_i \in \Omega_C$ . Then, we have

$$P\left\{s^*(\bar{B}_{\text{test}}, \bar{C}_{\text{test}}) \leq \text{Quantile}_{1-\alpha}\left(\frac{1}{|\mathcal{I}|} \sum_{i \in \mathcal{I}_{ca}(1) \cup \mathcal{I}_{ca}(0)} \delta_{s^*(\bar{B}_i, \bar{C}_i)} + \delta_{+\infty}\right) \middle| \bar{B} \in \Omega_C\right\} \geq 1 - \gamma.$$

Since we defined

$$\text{Quantile}_{1-\gamma} \left( \frac{1}{|\mathcal{I}|} \sum_{i \in \mathcal{I}_{ca}(a)} \delta_{s^*(\bar{B}_i, \bar{C}_i)} + \delta_{+\infty} \right) = \text{Quantile}_{1-\gamma}(\hat{F}^*) = \hat{q}_{1-\gamma}^*,$$

we obtain

$$\begin{aligned} P\{\bar{C}_{\text{test}} \subset \tilde{C}_C(\bar{B}_{\text{test}}) | \bar{B} \in \Omega_C\} &= P\left\{ \hat{m}^L(\bar{B}_{\text{test}}) - \hat{q}_{1-\gamma}^* \leq C_{\text{test}}^L, C_{\text{test}}^R \leq \hat{m}^R(\bar{B}_{\text{test}}) + \hat{q}_{1-\gamma}^* \mid \bar{B} \in \Omega_C \right\} \\ &= P\{\max\{\hat{m}^L(\bar{B}_{\text{test}}) - C_{\text{test}}^L, C_{\text{test}}^R - \hat{m}^R(\bar{B}_{\text{test}})\} \leq \hat{q}_{1-\gamma}^* | \bar{B} \in \Omega_C\} \\ &= P\{s^*(\bar{B}_{\text{test}}, \bar{C}_{\text{test}}) \leq \hat{q}_{1-\gamma}^* | \bar{B} \in \Omega_C\} \\ &\geq 1 - \gamma. \end{aligned}$$

Combined with the fact that  $P\{\bar{Y}_{\text{test}}(1) - \bar{Y}_{\text{test}}(0) \in C_{\text{test}} | \bar{B} \in \Omega_C\} \geq 1 - \alpha$ , we have

$$\begin{aligned} &P\{\bar{Y}_{\text{test}}(1) - \bar{Y}_{\text{test}}(0) \notin \tilde{C}_C(\bar{B}_{\text{test}}) | \bar{B} \in \Omega_C\} \\ &= P\{\bar{Y}_{\text{test}}(1) - \bar{Y}_{\text{test}}(0) \notin \tilde{C}_C(\bar{B}_{\text{test}}), \bar{C}_{\text{test}} \subset \tilde{C}_C(\bar{B}_{\text{test}}) | \bar{B} \in \Omega_C\} \\ &\quad + P\{\bar{Y}_{\text{test}}(1) - \bar{Y}_{\text{test}}(0) \notin \tilde{C}_C(\bar{B}_{\text{test}}), \bar{C}_{\text{test}} \not\subset \tilde{C}_C(\bar{B}_{\text{test}}) | \bar{B} \in \Omega_C\} \\ &\leq P\{\bar{Y}_{\text{test}}(1) - \bar{Y}_{\text{test}}(0) \notin \bar{C}_{\text{test}} | \bar{B} \in \Omega_C\} + P\{\bar{C}_{\text{test}} \not\subset \tilde{C}_C(\bar{B}_{\text{test}}) | \bar{B} \in \Omega_C\} \\ &\leq \alpha + \gamma, \end{aligned}$$

which completes the proof. □

## B.2 Individual-level treatment effect

**Theorem B.2.** *Assume Assumptions 1-3 and that  $(Y_{\text{test}}(1), Y_{\text{test}}(0), B_{\text{test}})$  is an arbitrary individual from a new cluster independently sampled from  $\mathcal{P}^W$ . Then, the  $\tilde{C}_I(B_{\text{test}})$  output*

---

**Algorithm B.2** Computing the conformal interval  $\tilde{C}_I(B)$  for individual-level treatment effects.

---

**Input:** Individual-level data  $\{(Y_{ij}, A_i, B_{ij}) : i = 1, \dots, m; j = 1, \dots, N_i\}$ , a test point  $B_{\text{test}}$ , a prediction model  $f_a(B)$  for  $Y(a)$ ,  $a \in \{0, 1\}$ , prediction models  $\{m^L(B), m^R(B)\}$  for the  $(\alpha/2, 1 - \alpha/2)$ -quantiles of  $Y(1) - Y(0)$ , a covariate-subgroup of interest  $\Omega_I$ , and levels  $(\alpha, \gamma)$ .

**Procedure:**

1. For  $a = 0, 1$ , randomly partition the arm- $a$  covariate-subgroup data  $\{(Y_{ij}, A_i, B_{ij}) : i = 1, \dots, m; j = 1, \dots, N_i; A_i = a; B_{ij} \in \Omega_I\}$  into a training fold  $\mathcal{O}_{tr}(a)$  and a calibration fold  $\mathcal{O}_{ca}(a)$  with index set  $\mathcal{I}_{ca}(a)$ .

2. Use the training fold to run Step 1 of Algorithm 2 of the main paper and obtain the  $(1 - \alpha)$  conformal interval  $\tilde{C}_{I,a}(B)$  for  $Y(a)$ ,  $a = 0, 1$ .

3. For each  $i = 1, \dots, m$ , define  $C_{ij} = A_i\{Y_{ij} - \tilde{C}_{I,0}(B_{ij})\} + (1 - A_i)\{\tilde{C}_{I,1}(B_{ij}) - Y_{ij}\}$  and denote  $C_{ij} = [C_{ij}^L, C_{ij}^R]$ .

4. Train prediction models  $m^L(B)$  for  $C^L$  and  $m^R(B)$  for  $C^R$  using all data in the training fold  $\{\mathcal{O}_{tr}(a) : a = 0, 1\}$ , and obtain the estimated models  $\hat{m}^L(B)$  and  $\hat{m}^R(B)$ .

5. For each  $(i, j) \in \mathcal{I}_{ca}(1) \cup \mathcal{I}_{ca}(0)$ , compute the non-conformity score

$$s^*(B_{ij}, C_{ij}) = \max\{\hat{m}^L(B_{ij}) - C_{ij}^L, C_{ij}^R - \hat{m}^R(B_{ij})\}.$$

6. Compute the  $1 - \gamma$  quantile  $\hat{q}_{1-\gamma}^*$  of the distribution

$$\hat{F}^* = \frac{1}{|\mathcal{I}_{ca}(1)| + |\mathcal{I}_{ca}(0)| + 1} \left\{ \sum_{i \in \mathcal{I}_{ca}(1) \cup \mathcal{I}_{ca}(0)} \frac{1}{\sum_{j=1}^{N_i} I\{B_{ij} \in \Omega_I\}} \sum_{j=1}^{N_i} I\{B_{ij} \in \Omega_I\} \delta_{s^*(B_{ij}, C_{ij})} + \delta_{+\infty} \right\}.$$

**Output:**  $\tilde{C}_C(B_{\text{test}}) = [\hat{m}^L(B_{\text{test}}) - \hat{q}_{1-\gamma}^*, \hat{m}^R(B_{\text{test}}) + \hat{q}_{1-\gamma}^*]$ .

---

by Algorithm B.2 satisfies

$$P\left\{Y_{\text{test}}(1) - Y_{\text{test}}(0) \in \tilde{C}_I(B_{\text{test}}) \mid B_{\text{test}} \in \Omega_I\right\} \geq 1 - \alpha - \gamma \quad (2)$$

for any set  $\Omega_I$  in the support of  $B_{\text{test}}$  with a positive measure.

*Proof of Theorem B.2.* Following the proof of Theorem 2, we have  $P(\tilde{Y}(a) \in \tilde{C}_{I,a}(\tilde{B})) \geq 1 - \alpha$ , where  $\tilde{Y}(a)$  and  $\tilde{B}$  represent the potential outcome  $Y(a)$  and covariates  $B$  given

$B \in \Omega_I$ . Since Assumption 2 implies that  $A$  is independent of  $(\tilde{Y}(a), \tilde{B})$ , then

$$\begin{aligned}
& P \left\{ \tilde{Y}(1) - \tilde{Y}(0) \in A\{Y - \tilde{C}_{C,0}(\tilde{B})\} + (1 - A)\{\tilde{C}_{C,1}(\tilde{B}) - \tilde{Y}\} \right\} \\
&= \sum_{a=0}^1 P \left\{ \tilde{Y}(a) \in \tilde{C}_{C,a}(\tilde{B}), A = a \right\} \\
&= \sum_{a=0}^1 P \left\{ \tilde{Y}(a) \in \tilde{C}_{C,a}(\tilde{B}) \right\} P(A = a) \\
&\geq 1 - \alpha.
\end{aligned}$$

Therefore, by defining  $\tilde{C}_{ij} = A_i\{\tilde{Y}_{ij} - \tilde{C}_{C,0}(\tilde{B}_{ij})\} + (1 - A_i)\{\tilde{C}_{C,1}(\tilde{B}_{ij}) - \tilde{Y}_{ij}\}$ , we have  $\tilde{C}_{ij} = [\tilde{C}_{ij}^L, \tilde{C}_{ij}^R]$  representing the  $(\alpha/2, 1 - \alpha/2)$ -quantile of  $\tilde{Y}_{ij}(1) - \tilde{Y}_{ij}(0)$ .

For the new cluster, in addition to sampling potential outcomes and covariates from  $\mathcal{P}^W$ , we independently generate  $A_{m+1}$  from  $\mathcal{P}^A$ , and compute  $\tilde{C}_{m+1,j} = A_{m+1}\{Y_{m+1,j} - \tilde{C}_{C,0}(\tilde{B}_{m+1,j})\} + (1 - A_{m+1})\{\tilde{C}_{C,1}(\tilde{B}_{m+1,j}) - \tilde{Y}_{m+1,j}\}$ . By construction,  $(\tilde{B}_{m+1,j}, \tilde{C}_{m+1,j})$  is independently and identically distributed as  $(\tilde{B}_{ij}, \tilde{C}_{ij})$ . We observe that  $\tilde{C}_{C,a}, \hat{m}^L, \hat{m}^R$  are all functions of the training folds  $\{\mathcal{O}_{tr}(a) : a = 0, 1\}$ , which are independent of the calibration data and test data. Denoting  $\mathcal{I} = \mathcal{I}_{ca}(1) \cup \mathcal{I}_{ca}(0) \cup \{\text{test}\}$ , by Assumptions 1-2,  $\{s^*(\tilde{B}_i, \tilde{C}_i), i \in \mathcal{I}\}$  are i.i.d. conditioning on the training folds and  $\tilde{B}_i \in \Omega_C$ . Then, we have

$$P \left\{ s^*(\tilde{B}_{m+1,1}, \tilde{C}_{m+1,1}) \leq \text{Quantile}_{1-\gamma} \left( \frac{1}{|\mathcal{I}|} \sum_{i \in \mathcal{I}_{ca}(1) \cup \mathcal{I}_{ca}(0)} \frac{1}{M_i} \sum_{j=1}^{M_i} \delta_{s^*(\tilde{B}_{ij}, \tilde{C}_{ij})} + \delta_{+\infty} \right) \right\} \geq 1 - \gamma.$$

By the definition of  $\hat{F}^*$ , we have

$$\text{Quantile}_{1-\gamma} \left( \frac{1}{|\mathcal{I}|} \sum_{i \in \mathcal{I}_{ca}(1) \cup \mathcal{I}_{ca}(0)} \frac{1}{M_i} \sum_{j=1}^{M_i} \delta_{s^*(\tilde{B}_{ij}, \tilde{C}_{ij})} + \delta_{+\infty} \right) = \text{Quantile}_{1-\gamma}(\hat{F}^*) = \hat{q}_{1-\gamma}^*,$$



we obtain

$$\begin{aligned}
P\{\tilde{C}_{m+1,1} \subset \tilde{C}_C(\tilde{B}_{m+1,1})\} &= P\left\{\hat{m}^L(\tilde{B}_{m+1,1}) - \hat{q}_{1-\gamma}^* \leq C_{m+1,1}^L, C_{m+1,1}^R \leq \hat{m}^R(\tilde{B}_{m+1,1}) + \hat{q}_{1-\gamma}^*\right\} \\
&= P\{\max\{\hat{m}^L(\tilde{B}_{m+1,1}) - C_{m+1,1}^L, C_{m+1,1}^R - \hat{m}^R(\tilde{B}_{m+1,1})\} \leq \hat{q}_{1-\gamma}^*\} \\
&= P(s^*(\tilde{B}_{m+1,1}, \tilde{C}_{m+1,1}) \leq \hat{q}_{1-\gamma}^*) \\
&\geq 1 - \gamma.
\end{aligned}$$

Combined with the fact that  $P\{\tilde{Y}_{m+1,1}(1) - \tilde{Y}_{m+1,1}(0) \in C_{m+1,1}\} \geq 1 - \gamma$ , we have

$$\begin{aligned}
&P\{\tilde{Y}_{m+1,1}(1) - \tilde{Y}_{m+1,1}(0) \notin \tilde{C}_C(\tilde{B}_{m+1,1})\} \\
&= P\{\tilde{Y}_{m+1,1}(1) - \tilde{Y}_{m+1,1}(0) \notin \tilde{C}_C(\tilde{B}_{m+1,1}), \tilde{C}_{m+1,1} \subset \tilde{C}_C(\tilde{B}_{m+1,1})\} \\
&\quad + P\{\tilde{Y}_{m+1,1}(1) - \tilde{Y}_{m+1,1}(0) \notin \tilde{C}_C(\tilde{B}_{m+1,1}), \tilde{C}_{m+1,1} \not\subset \tilde{C}_C(\tilde{B}_{m+1,1})\} \\
&\leq P\{\tilde{Y}_{m+1,1}(1) - \tilde{Y}_{m+1,1}(0) \notin \tilde{C}_{m+1,1}\} + P\{\tilde{C}_{m+1,1} \not\subset \tilde{C}_C(\tilde{B}_{m+1,1})\} \\
&\leq \alpha + \gamma.
\end{aligned}$$

Finally, by Lemma 1 (c),  $P\{\tilde{Y}_{m+1,1}(1) - \tilde{Y}_{m+1,1}(0) \notin \tilde{C}_C(\tilde{B}_{m+1,1})\} = P\{Y_{\text{test}}(1) - Y_{\text{test}}(0) \notin \tilde{C}_C(B_{\text{test}}) | B_{\text{test}} \in \Omega_I\}$ , which completes the proof.  $\square$

## C Additional simulations

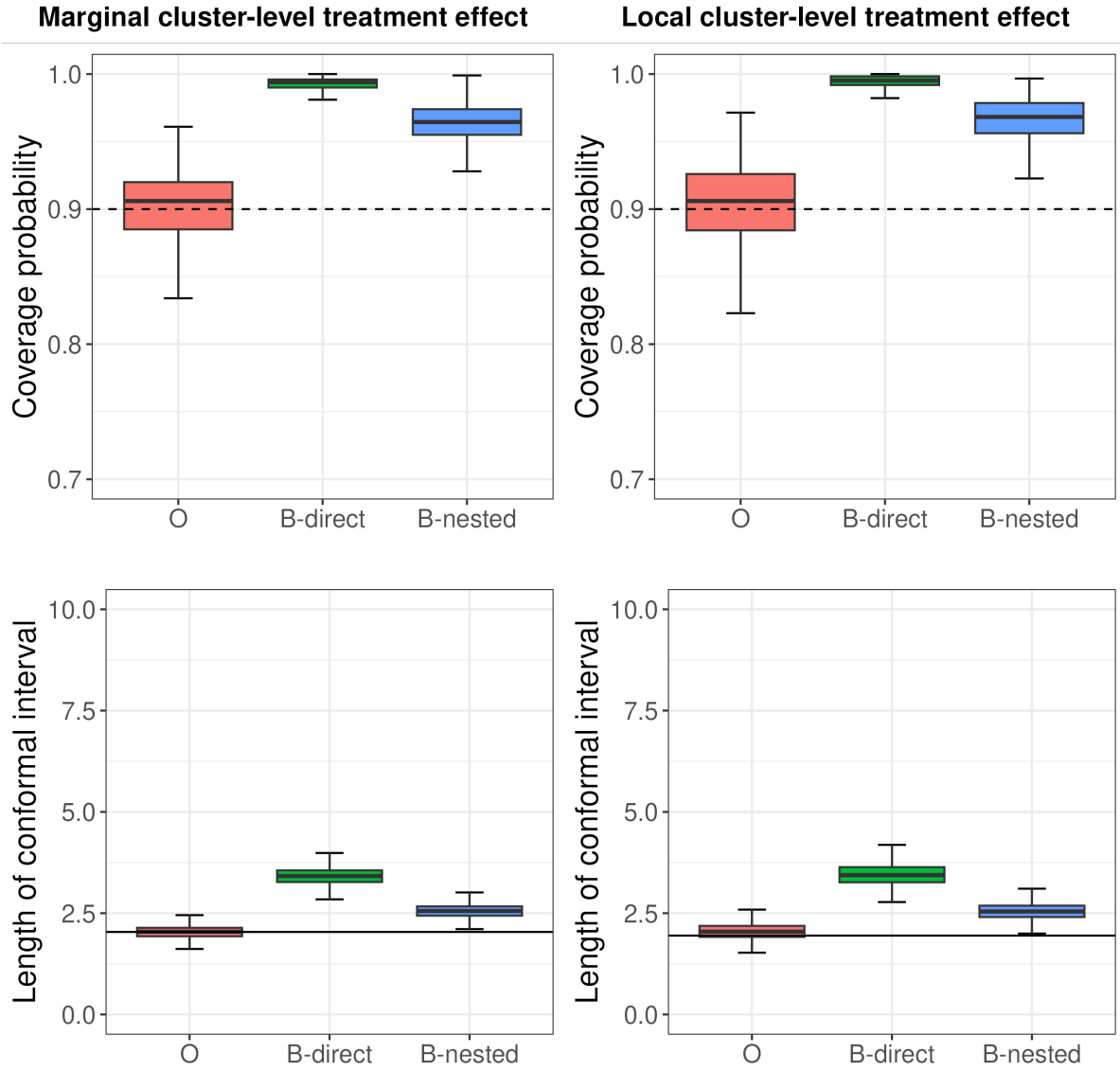


Figure 1: Simulation results (boxplot) for the marginal (left column) and local (right column, conditioning on  $\{R_{i1} \geq 2, R_{i2} = 1\}$ ) cluster-level treatment effects with  $m = 500$ . In the upper panels, the dashed line is the target 90% coverage probability. In the lower panels, the solid line is the oracle length of conformal intervals, computed as the average length between the  $(\alpha/2, 1 - \alpha/2)$ -quantiles of  $\bar{Y}(1) - \bar{Y}(0)$  among test data.

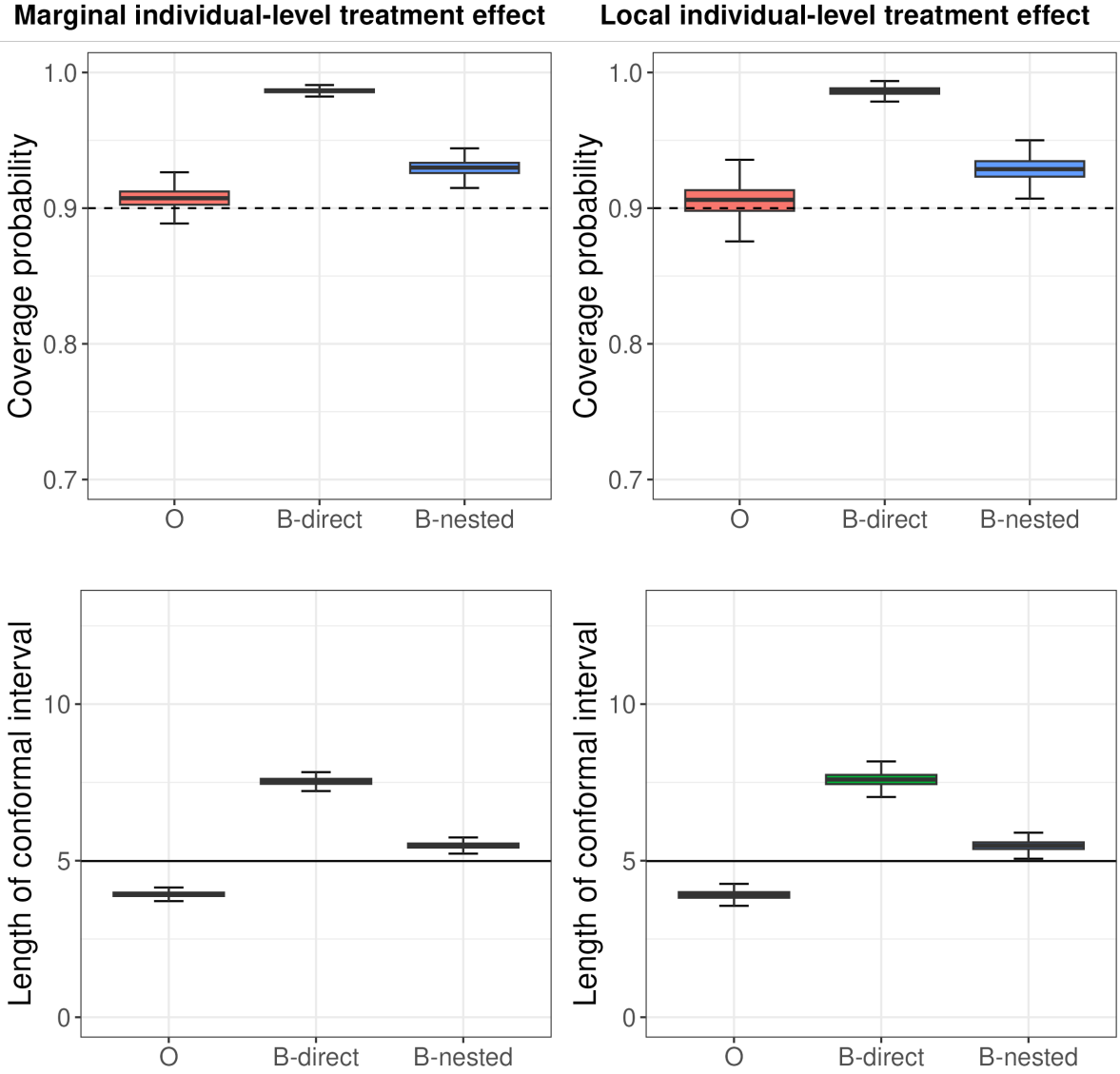


Figure 2: Simulation results (boxplot) for the marginal (left column) and local (right column, conditioning on  $\{|X_{ij1}| < 0.5\}$ ) individual-level treatment effects with  $m = 500$ . In the upper panels, the dashed line is the target 90% coverage probability. In the lower panels, the solid line is the oracle length of conformal intervals, computed as the average length between the  $(\alpha/2, 1 - \alpha/2)$ -quantiles of  $Y(1) - Y(0)$  among test data.

Table 1: Summary of simulation results for 80% and 90% conformal intervals given  $m = 30$  clusters with linear regression as the prediction model. For both coverage probability and length of intervals, we report their averages and standard errors. The local treatment effect is conditioned on  $|X_{ij1}| < 0.5$ .

Treatment effects	Methods	$\alpha = 0.2$		$\alpha = 0.1$	
		Coverage probability	Length of intervals	Coverage probability	Length of intervals
Marginal cluster-level	O	0.821(0.095)	5.149(4.266)	0.915(0.071)	7.457(8.898)
	B-direct	0.999(0.007)	10.310(8.526)	1.000(0.001)	14.910(8.017)
Marginal individual-level	O	0.865(0.044)	4.966(1.114)	0.972(0.020)	7.636(1.636)
	B-direct	0.994(0.006)	9.706(2.076)	1.000(0.000)	15.027(3.010)
Local individual-level	O	0.861(0.057)	4.722(1.067)	0.974(0.025)	7.556(1.725)
	B-direct	0.991(0.009)	9.229(1.877)	1.000(0.000)	14.700(2.893)